Monthly Weather Review

VOLUME 99, NUMBER 2

FEBRUARY 1971

UDC 551.509.616.001.57(759)"1968.05"

1968 FLORIDA CUMULUS SEEDING EXPERIMENT: NUMERICAL MODEL RESULTS

JOANNE SIMPSON and VICTOR WIGGERT

Experimental Meteorology Laboratory, NOAA, Miami, Fla.

ABSTRACT

A one-dimensional numerical cumulus model was tested against data from a randomized seeding experiment made in South Florida in 1968. Fourteen GO clouds were studied. Nine were seeded by pyrotechnics with 1 kg of silver iodide each, while five were studied identically as controls.

Various seeding subroutines and assumptions regarding the ice phase are compared. The experimental aircraft data are used to guide the modeling assumptions and to select the most realistic ones. Seedability and seeding effect correlate to 0.96 for seeded clouds in the three best models. A high correlation is found between seedability and radar-measured rainfall increase from seeding. Also, a high correlation is found between model predictions of the difference in precipitation fallout between seeded and control clouds and the measured rainfall differences, although the model predictions are much smaller in magnitude. A calculation is undertaken showing that coalescence within the cloud body on descent of the raindrops easily accounts for the discrepancy.

The model predictions for each GO cloud are discussed in comparison with actual measurements on the cloud.

The 1968 experiment was found to subdivide into two periods, one fair and one disturbed, with quite different effects of seeding. The two periods and corresponding cloud behavior are compared. It is concluded that the disturbed period was less favorable for seeding because of higher unseeded cloud growth and strong wind shear. Implications of this result for future modeling efforts are discussed.

CONTENTS

1. INTRODUCTION

In May 1968, the third in a series of individual cumulus seeding experiments took place in South Florida. The series involved massive seeding of single cumuli from above with airborne silver iodide pyrotechnics. The purpose of the seeding was to induce dynamic invigoration of the cloud's updraft structure by means of releasing the latent heat content of its supercooled water. The program was conducted by ESSA's Experimental Meteorology Laboratory together with the Atmospheric Physics Branch of the Naval Research Laboratory. Other participants included the University of Miami's Radar Laboratory, Meteorology Research, Inc., the National Hurricane Center, and the Air Weather Service of the U.S. Air Force. The first experimental series based on this philosophy took place in the Caribbean in 1963 (Malkus and Simpson 1964). The results suggested that, under specifiable conditions, massive seeding can cause some cumulus clouds to grow explosively. Although not conclusive, due to lack of randomization, this first experiment stimulated alteration of an existing cumulus model (Levine 1959, Malkus 1960) to include a "seeding subroutine" that simulated the dynamic effects of seeding (Simpson et al. 1965). This model, called EMB 65, was used in connection with a randomized, more extensive seeding experiment in 1965, also in the Caribbean.

The 1965 experiment showed conclusively that seeding causes vertical cloud growth under predictable conditions

and that the numerical model had considerable skill in predicting both seeded and unseeded cloud tops to an accuracy within several hundred meters (Simpson et al. 1967). In 1965, one-third of the seeded clouds grew explosively and, it was suspected, rained more than if they had not been seeded. However, no rainfall measurements were possible over the Caribbean Sea. Furthermore, the EMB 65 version of the model arbitrarily dropped one-half the condensate from the cloud tower and hence ignored the feedback between the dynamics of the cloud and its precipitation physics.

Following the 1965 experiment, the numerical model was improved by the addition of equations parameterizing the growth and fallout of precipitation. The precipitation growth equations were based on the work of Kessler (1965) and Berry (1968). A hierarchy of seeding subroutines, with different hypotheses concerning ice processes, were tested against the 1965 data. This model hierarchy was called the EMB 68 series; its development and first testing have been described by Simpson and Wiggert (1969).

The 1965 data, however, did not include enough internal cloud physics measurements to satisfactorily test or improve the model beyond a certain point. Hence the experimental aircraft were equipped with cloud particle samplers for the third experiment. The main purpose of the 1968 experiment was to relate the dynamics to the precipitation physics of the cloud, through improved measurements jointly with improved modeling. The purpose of this paper is to use the 1968 measurements first to improve the model, then to test the improved model with simultaneous aircraft, photographic, and radar observations, and finally to use all these observations, in the context of the model, to construct a picture of the dynamics and precipitation history of individual seeded and unseeded clouds.

2. SUMMARY OF THE 1968 FLORIDA EXPERIMENT

Improved pyrotechnics permitted moving the experimental site to the South Florida land area within the range of the University of Miami's calibrated radar. The development, testing, and use of the pyrotechnics have been discussed by Simpson et al. (1970*b*) who also describe the field design of the 1968 experiment together with the preliminary results.

The EMB 68 model was run (with the 1200 GMT Miami radiosonde) in real time each morning in advance of an operation, with a hierarchy of assumed tower radii. If predicted seedabilities were small, the operation was cancelled, thus avoiding all but one "no growth" case following seeding. Altogether, 19 GO clouds were studied between May 15 and June 1, 1968, located as shown in figure 1. Sealed envelopes[1] opened on the seeder aircraft indicated that 14 of these GO clouds were to be seeded and five were to be left unseeded but penetrated identically as controls. Following the seeding run, the seeded clouds grew an average of 11,400 ft more than the controls, a difference significant at the 0.5-percent level.

The precipitation evaluation using the ground-based calibrated radar has been described by Woodley (1970*a*). While the precipitation varied widely from cloud to cloud and from day to day, on the average the seeded clouds precipitated twice as much as the controls with the difference averaging 140 acre-ft by 40 min after seeding, a substantial amount of water. To augment the small sample of control clouds, Woodley devised an objective scheme of choosing additional "radar control" clouds from the nose camera record on the seeder aircraft. These clouds were then located on the radar film, and their precipitation evaluated in the same manner as that of the actual GO clouds. Their inclusion did not change the rainfall difference between seeded and control clouds. The latter was shown to be significant at the 5- to 20-percent level, depending on the statistical test used.

The radar evaluation of rainfall was supported by a radar-rain gage comparison reported by Woodley and Herndon (1970). Total shower rainfall measured by recording gages was compared with estimates derived from the Miami Z–R relation (Gerrish and Hiser 1965) in conjunction with radar reflectivity measurements. The radar and rain gage estimates were highly correlated (+0.93, significant at the 1-percent level) and differed an average between 8 and 30 percent.

No seeded clouds were available for the radar-rain gage comparison, but the missing link was provided by the experimental aircraft foil sampler records (Takeuchi 1969). Precipitation samples with the foil were obtained in most GO clouds at cloud base and at 19,000-ft pressure altitude. No significant difference in precipitation spectrum or rainfall rate was found between seeded and control clouds at either level. First, this result demonstrates that the Miami Z–R relation is equally valid for seeded as for unseeded clouds; and hence the radar-measured differences in precipitation exist regardless of possible error in absolute amounts. Second, this result indirectly confirms the dynamic seeding hypothesis, namely that it is the longer life and larger cloud that causes the increased precipitation rather than any change in drop spectrum or rainfall rate, as prescribed by older seeding theories. This postulate was hard to confirm by direct measurement because 58 percent of the seeded cloud echoes (generally the larger ones) merged with neighboring echoes while still active. Even with this unfortunate population reduction, seeded echo lifetimes exceeded those of the controls (only one merger) by 39 percent, and the areas of seeded echoes exceeded those of control echoes by 47 percent during the first 40 min after the seeding run. Furthermore, a cloud's rain production following seeding was highly correlated to its vertical growth (Woodley 1970*a*).

Additional reports already completed on the 1968 results concentrate mainly on 3 days, namely May 16 (Simpson and Woodley 1969), May 19 (Woodley 1970b), and May 30 (Woodley and Powell 1970). In these partic-

[1] Weighted 65 to 35 in favor of the "seed" instruction

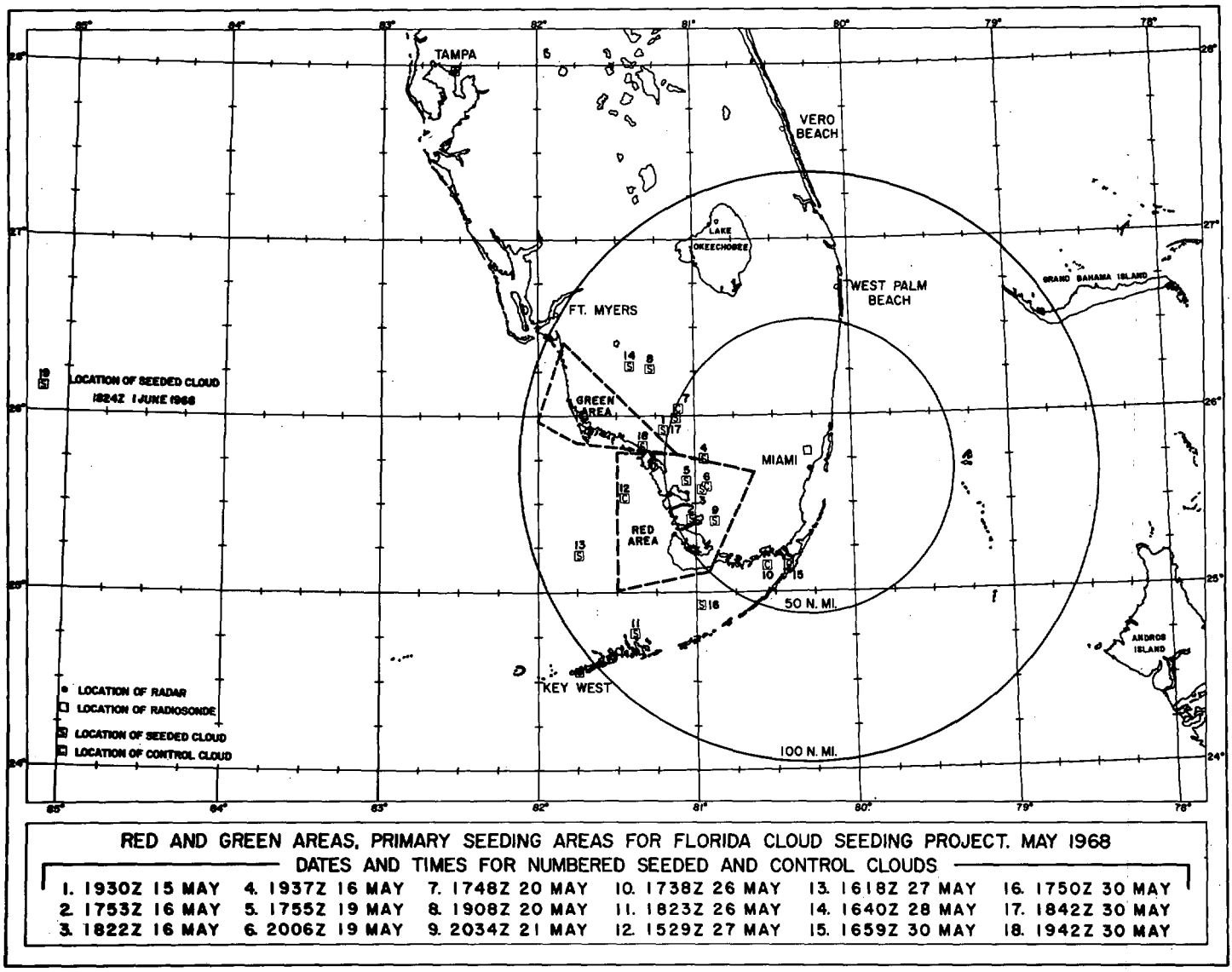

RED AND GREEN AREAS, PRIMARY SEEDING AREAS FOR FLORIDA CLOUD SEEDING PROJECT. MAY 1968

DATES AND TIMES FOR NUMBERED SEEDED AND CONTROL CLOUDS

1. 1930Z 15 MAY	4. 1937Z 16 MAY	7. 1748Z 20 MAY	10. 1738Z 26 MAY	13. 1618Z 27 MAY	16. 1750Z 30 MAY
2. 1753Z 16 MAY	5. 1755Z 19 MAY	8. 1908Z 20 MAY	11. 1823Z 26 MAY	14. 1640Z 28 MAY	17. 1842Z 30 MAY
3. 1822Z 16 MAY	6. 2006Z 19 MAY	9. 2034Z 21 MAY	12. 1529Z 27 MAY	15. 1659Z 30 MAY	18. 1942Z 30 MAY

FIGURE 1.—Location of GO clouds in the Florida 1968 cumulus seeding experiment. The seeded clouds are denoted by S and the control clouds by C. The clouds are numbered in order of study corresponding to numbers in the tables and text. The dashed areas are so-called "red" and "green" areas, set aside by the Federal Aviation Administration as the main land areas to be used in the experiment.

ularly interesting cases, detailed case studies of the cloud have been prepared using aircraft penetrations, radar, modeling, and airborne photogrammetry following a method devised by Herrera-Cantilo (1969). On May 16, Woodley and Fernandez-Partagas (1969) studied synoptic and mesoscale conditions on the Florida Peninsula with the aid of satellite and airborne photography, while Ruskin et al. (1969) have prepared a detailed cloud physics study with emphasis on cloud condensation nucleus populations and their relationship to seeding potential. The synoptic, general circulation, and large-scale disturbance context of the whole experiment has been analyzed for each day by Fernandez-Partagas (1969), while the large-scale effects on rainfall of the seeding have been investigated by Woodley et al. (1969).

3. DEVELOPMENT OF THE NUMERICAL MODEL

The early development of the model was reported by Simpson et al. (1965). Its further development up to the 1968 experiment has been described in detail in a paper by Simpson and Wiggert (1969) hereinafter referred to as I. Briefly, we treat a one-dimensional parameterized model of the active rising phase of an individual cumulus tower. The cloud tower is idealized as either a jet, a buoyant rising plume, a "thermal" with vortical internal circulation, or a hybrid of these forms. With this basic postulate, the differential equation for the rate of rise of the tower center is shown to be

$$\frac{dw}{dt}=w\frac{dw}{dz}=\frac{d}{dz}\left(\frac{w^2}{2}\right)=\frac{gB}{1+\gamma}-\frac{9}{32}\frac{K_2}{R}w^2 \qquad (1)$$

where z is height and t is time, gB is the buoyancy force per unit mass, γ is the virtual mass coefficient, K_2 is the entrainment coefficient, and R is the radius or horizontal half-width of the cumulus tower.

The buoyancy term is evaluated as

$$\text{buoyancy}=gB=\frac{g[\Delta T_v-\Delta T_v(\text{LWC})]}{T_v(\text{env})} \tag{2}$$

where ΔT_v is the virtual temperature difference between tower and surroundings and ΔT_v (LWC) is the reduction due to weight of suspended hydrometeors, as formulated by Saunders (1957), namely:

$$\Delta T_v(\text{LWC})=T_v \cdot r_{cw} \tag{3}$$

where T_v is the virtual temperature in the cloud and r_{cw} is its hydrometeor content in grams per gram.

The values of K_2 and γ are taken as 0.65 and 0.5, respectively, as explained in I. These values are equal or close to laboratory values and have been checked by aircraft measurements. R is measured by photogrammetry and is usually assumed constant with height. Other necessary input data are an environment temperature-humidity sounding and cloud base height and conditions. The latter are saturation at ambient temperature, which is roughly verified by cloud base measurements over and near Florida. The value of the initial rise rate has been shown (Andrews 1964) to make negligible difference; we have chosen 1 m s^{-1}.

First, an entrainment calculation is performed on the computer proceeding from cloud base upward between sounding points and assuming in-cloud saturation with respect to either water or ice. Output variables are cloud temperature, specific humidity, and liquid water condensed. These cloud properties are then available to calculate buoyancies at any interpolated intervals to integrate eq (1) in ascending steps. For completing gB and undertaking the integration, it only remains to specify a growth and fallout scheme for precipitation. The maximum height achieved by the tower center is defined to be that level where w goes to zero. The tower radius must be added to compare with the height of the measured cloud top.

The equations for the growth and fallout of precipitation have been described in detail in I. Briefly, all water is first condensed as cloud water, with small drop size (roughly 5–30 μm) and negligible terminal velocity. Then a process called autoconversion begins. This involves the formation of precipitation particles either by the aggregation of several cloud particles or by the action of giant salt nuclei, or similar processes. In this study, we use an autoconversion equation developed theoretically by Berry (1968) from a model of initial growth by condensation and coalescence of cloud-sized particles with each other, namely:

$$\frac{dM}{dt}(\text{autoconversion})=\frac{m^2}{60\left(5+\frac{0.0366}{m}\frac{N_b}{D_b}\right)}\ \text{g m}^{-3}\ \text{s}^{-1} \tag{4}$$

where dM/dt is the rate of growth of precipitation water content M (in g m^{-3}) and m is cloud water content (in g m^{-3}). The boundary between cloud water m and precipitation water M was defined in I as a drop diameter of about 200 μm. The early droplet spectrum near cloud base has a number concentration of N_b drops per cubic centimeter and a relative dispersion D_b due to the condensation spectrum. The relative dispersion D_b is defined as

$$D_b=\frac{\text{standard deviation of droplet radii}}{\text{mean droplet radius}}.$$

An important feature of Berry's eq (4) is that a different autoconversion rate is permitted for maritime and for continental clouds. Ruskin et al. (1969) have reported cloud base counts of condensation nuclei during the Florida experiment and point out that the degree of continentality may have an important effect on seeding results. Using their measurements, we assume for the 12 GO clouds over the Florida Peninsula a drop concentration of 500 cm^{-3} and a relative dispersion of $D_b=0.146$. With this set of parameters, use of eq (4) is called "Berry Florida Conversion." For the seven GO clouds over the ocean, we have taken a drop concentration of 50 cm^{-3} at cloud base and a relative dispersion of 0.366. With this set of parameters, use of eq (4) is called "Berry Marine Conversion."

Once precipitation is formed, the precipitation drops will grow predominantly by collection of the small cloud drops. Our coalescence or collection equation is that derived by Kessler (1965, 1969) for a continuous collection process. A fundamental assumption is that the precipitation spectrum can be described by an equation of the form

$$n_D=n_0e^{-\lambda D} \tag{5}$$

where D is the diameter, $n_D\delta D$ is the number of drops with diameters in the range between D and $D+\delta D$ in unit volume of space, and n_0 is the value of n_D for $D=0$. That raindrop spectra followed an equation of this form was originally proposed by Marshall and Palmer (1948) from observations of showers at the ground. It has been verified for active cloud towers by Mee and Takeuchi (1968) in the Tropics and by Braham (1968) and others in mid-latitudes.

In eq (5), the exponent λ is related to the precipitation water content by integrating over all diameters to obtain

$$\lambda=42.1\ n_0^{0.25}M^{-0.25} \quad \text{or} \quad \lambda=\frac{3.67}{D_0} \tag{6}$$

in the gram-meter-second system of units. D_0 is the median volume drop diameter or the diameter that divides the distribution into parts of equal water content.

We use the following equation (Kessler 1965) for the terminal velocity of raindrops, namely:

$$V=-130\ D^{1/2}\ \text{m s}^{-1} \quad (D \text{ in meters}). \tag{7}$$

Using eq (5–7) and physical reasoning, Kessler obtains a

collection equation, namely:

$$\frac{dM}{dt}\,(\text{collection}) = 6.96\times10^{-4} E n_0^{0.125} m M^{0.875}\ \text{g m}^{-3}\ \text{s}^{-1} \tag{8}$$

where E is the collection efficiency of precipitation particles for cloud particles.

For the fallout scheme, we consider the average precipitation particle to be located at the tower center and to fall with terminal velocity V_0 for the median volume drop diameter D_0. It leaves the vortically circulating portion of the tower after falling through a height interval R. The fractional fallout of precipitation M in each height interval is therefore the ratio of the time for the tower to rise through the vertical height step over which the integration is being made (50 m) to the time for the median volume diameter drop to fall through one radius.

From this point, the water budgeting is straightforward. All water condensed in the entrainment calculation in each vertical interval $(z_2-z_1)=dz$ is first put into cloud water m. Then autoconversion and collection calculations are applied to obtain ΔM in the interval where $dt=dz/w_1$. Then ΔM is added to M and subtracted from m. The fallout is summed with height in a separate column to give later the total fallout of precipitation from the tower. The final sum of $m+M$ after conversion, collection, and fallout is used in the buoyancy correction to calculate w_2; and this same sum is then exported upward to repeat the water budget in the next height interval.

Once the precipitation water content and spectrum are defined, the radar reflectivity of the rising tower is also readily predicted, namely:

$$Z=3.2\times10^{9} n_0^{-0.75} M^{1.75}\quad (\text{mm}^6\ \text{m}^{-3}). \tag{9}$$

For liquid clouds, it only remains to specify n_0 and E which are now fairly well known from measurements. As explained in I, we take $n_0=10^7$ m^{-4} and $E=1$ for water clouds.

4. SEEDING SUBROUTINE AND MODEL HIERARCHY

The effects of seeding are introduced linearly between the levels of −4°C and −8°C in the model. The latent heat of fusion is released in this interval and adds to the cloud temperature. The cloud also goes from water saturation to ice saturation in this interval, adding a comparable temperature increment due to the depositional heating resulting from the excess water vapor depositing out into ice. The basic rationale for this procedure was established by Simpson et al. (1965) and Andrews (1964). It remains to specify what fraction of the cloud's calculated H_2O content at −4°C is to be frozen and how the collection efficiency, precipitation spectrum, and terminal velocity law alter when the hydrometeors are converted into ice.

In preparing I, we had no direct observational information on any of these important points except for vastly conflicting evidence about ice-for-ice collection efficiency. We therefore took an unchanged precipitation spectrum (with $n_0=10^7$ m^{-4}) for ice and considered 13 different seeding subroutines labeled EMB 68 A to EMB 68 M, in which the ice parameters were varied one at a time within wide but physically reasonable limits. Each subroutine was then run with the data from the 12 seeded clouds studied in the 1965 seeding experiment, and the height predictions of each were tested against observations in I.

TABLE 1.—*Properties of two seeding models used with 1965 data*

Model	TLWC (%)	E_{ice}	V_T	$\lvert\bar{e}\rvert$ (m)	$R_{S,EF}$	n_0 (m^{-4})
A	100	0.1	0.20	520	0.93	10^7
K	80	1.0	.20	430	.94	10^7

Properties of two of the better subroutines are shown in table 1. In the table, the column labeled TLWC gives the percentage of the water at −4°C that is frozen in the seeding subroutine; E_{ice} is the ice collection efficiency; the fraction in the column marked V_T is the fraction used in the terminal velocity law (7) for the reduced fall velocity of ice particles relative to that of water particles; $|\bar{e}|$ is the average absolute error in height prediction; and $R_{S,EF}$ is the correlation between seedability and seeding effect, which would be unity if the model and data were perfect (see next section for fuller discussion).

In the model hierarchy, TLWC was varied between 60 and 100 percent; E_{ice} was varied between 0.1 and 2.0; and the fraction of V_T was varied between 0.20 and 1.0. Briefly, results were relatively insensitive to variations in E_{ice}. However, it proved necessary to reduce the terminal velocity of ice particles drastically to reduce vertical momentum sufficiently not to overpredict cloud tops. Model A was the version used in the real time predictions in advance of each seeding operation; but the later developed model K appeared to give slightly better height predictions, so that it was originally planned to use K in the post-analysis of the 1968 data.

However, the 1968 cloud penetrations shed a new light on modeling parameters. Ice spectra were constructed from the foil sampler flown at 19,000 ft. Results are compared with a typical water spectrum in figures 2 and 3. Equation (5) still approximates the actual ice spectrum very well; but n_0 is about 10^8 m^{-4}, one order of magnitude higher than in liquid clouds. This means more smaller particles and hence a smaller V_0 for the same precipitation content. The foil sampler records, taken together with other water content measurements, also showed that as much as 40 percent of the mass of the cloud hydrometeors was frozen at the time of seeding (see table 7 and discussion). Beyond that, from the 1968 experiment, we had in hand Formvar[2] ice particle replicas quite similar to those on which Braham (1964) had made terminal fall speed measurements. He found that the ice terminal velocities were about 0.7 times the terminal velocities of water drops of equivalent mass. The specific gravity of the ice pellets

[2] Mention of a commercial product does not constitute an endorsement.

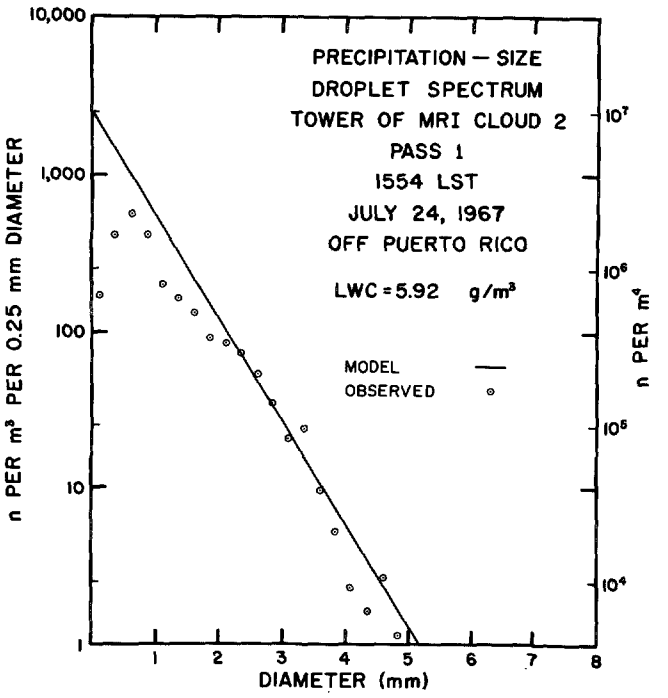

FIGURE 2.—Typical liquid precipitation spectrum in the actively rising tower of a tropical cumulus. Measurement was made with a foil sampler flown at 6 km through a completely unfrozen cloud. The apparent deficiency of droplets of diameters less than 0.5 mm may be a measurement problem.

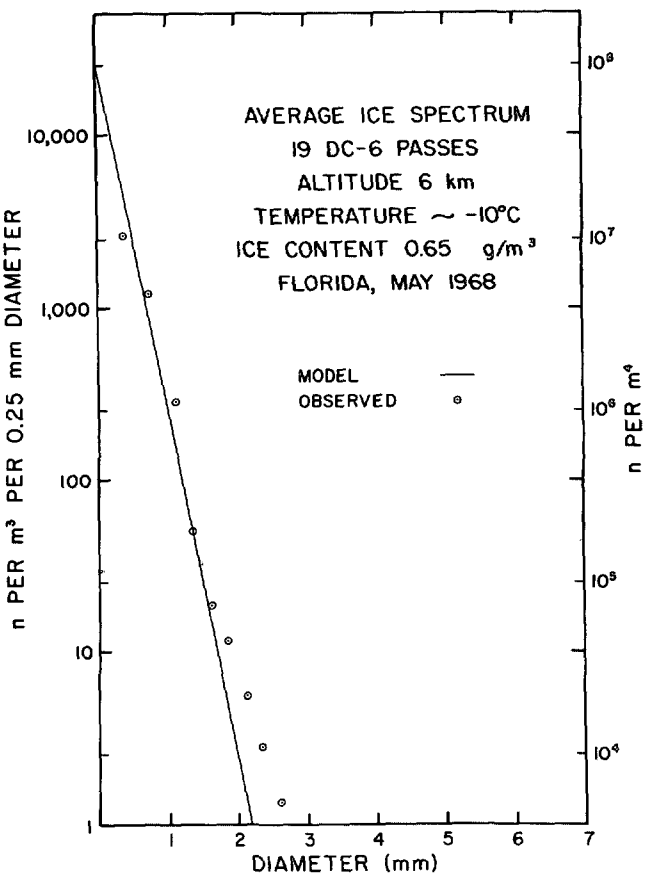

FIGURE 3.—Average ice spectrum (for precipitation size particles) through Florida cumuli in May 1968. All foil sampler records have been averaged; only about one-fourth of the passes were through an active tower.

was measured between 0.87 to 0.91, and we shall therefore neglect the small density difference between ice and water.

As a result of these new observations, models N, O, and P were developed as specified in table 2. It soon became clear that model N seriously overpredicts top heights. Hence models K, O, and P are selected for comparison with the 1968 observations. It should be recalled in examining the comparison that model P comprises the most realistic set of parameters.

TABLE 2.—*Models based on new data for use with 1968 observations*

Model	TLWC (%)	E_{ice}	V_T	n_0 (m^{-4})
N	80	1.0	1.0	10^8
O	80	1.0	.5	10^8
P	60	1.0	.7	10^8

5. MODEL COMPARISONS WITH THE 1968 OBSERVATIONS

To run the numerical model for each GO cloud of 1968, we found it necessary first to select the sounding most characteristic of the cloud environment and to measure the tower radius R. During the operational period, rawinsondes were available from both Miami and Key West (fig. 1) at 0000, 1200, and 1800 GMT. On many days, special Air Force dropsondes were made over water, but as near as possible to the experimental cloud. The sounding best representing each cloud environment was selected using the approaching runs from the monitoring aircraft at 19,000 ft and cloud base, combined with the seeder aircraft temperatures at higher levels. The sounding giving the best fit to these observations was chosen; it was usually, but not invariably, the sounding closest to the cloud in space and time.

The cloud tower radius was measured with the method of Herrera-Cantilo (1969). The photogrammetric measurements were made using the side camera film from the 19,000-ft ESSA DC–6 aircraft at the time closest to seeding time that the tower was visible on either side camera, generally within 2 to 3 min after seeding. On several days (May 16, 19, 30), a complete photogrammetric time history of top heights and radii were made. For cloud 3 and particularly cloud 4 on May 16, the measured tower expansion was large after seeding, and it has been incorporated in special model studies discussed by Simpson and Woodley (1969) and shown in figures 10 and 11 herein. However, since this precision was not possible on many GO clouds due to often obscured visibility on the photographs, the model comparisons and statistics here were made based on computations using the radii given in table 3 without any expansion or alteration.

Seeded cloud numbers are in circles, and control cloud numbers are in boxes. The average radius of seeded cloud towers was 994 m; that of control cloud towers was 920 m.

TABLE 3.—*Tower radius and sounding used for each GO cloud in Florida (1968)*

Cloud	Date	Radius (m)	Sounding	GMT
①	May 15	1300	USAF drop	2000
②	16	650	Miami radiosonde	1800
③	16	1000	Miami radiosonde	1800
④	16	1000	Miami radiosonde	1800
⑤	19	1000	USAF drop	1900
⑥	19	850	Miami radiosonde	1800
⑦	20	1000	Miami radiosonde	1800
⑧	20	1200	Miami radiosonde	1800
⑨	21	1200	USAF drop	2050
⑩	26	850	Miami radiosonde	1800
⑪	26	900	Key West radiosonde	0000 (27th)
⑫	27	1000	Miami radiosonde	1200
⑬	27	1000	Miami radiosonde	1200
⑭	28	750	Miami radiosonde	1800
⑮	30	900	Miami radiosonde	1800
⑯	30	875	Miami radiosonde	1800
⑰	30	1100	Miami radiosonde	1800
⑱	30	1100	Miami radiosonde	1800
⑲	June 1	850	USAF drop	1700

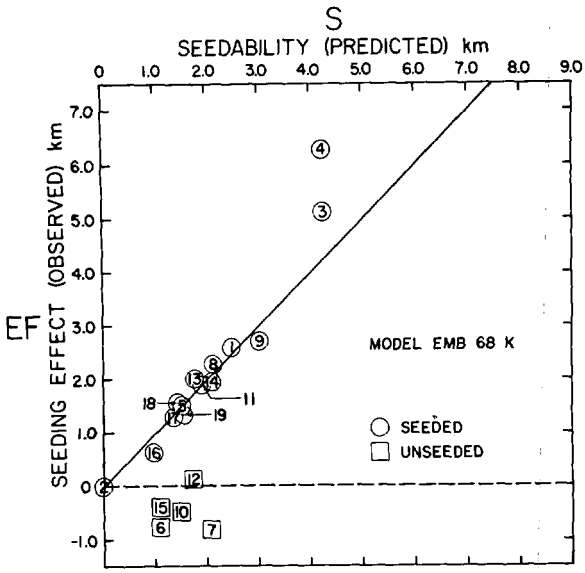

FIGURE 4.—Seedability versus seeding effect for model EMB 68 K.

The difference is not statistically significant. It is unfortunate that there were so few control clouds in 1968. Furthermore, on 2 of the 5 days when there was both a control cloud and one or more seeded clouds, the clouds were so far apart in space that a different sounding applied to the environment of control and seeded cloud.

The first comparative test to make with the models is that of plotting seedability versus seeding effect for both seeded and control clouds. Seedability is defined as the amount (in km) that the predicted maximum top height of the seeded cloud exceeds the predicted maximum unseeded top height of the same cloud. Seeding effect is defined as the amount (in km) that the observed maximum top height of the cloud exceeds the predicted maximum unseeded top height. If the model and data were perfect, seeded clouds would have equal seedability and seeding effect and hence should lie along the straight line with slope one, while the control clouds should show no seeding effect regardless of how large their seedability and hence should lie along the straight line with slope zero.

Figures 4–6 show the seedability-seeding effect diagrams for seeded models K, O, and P and for unseeded clouds (no difference between models).

For each model, the correlation between seeding effect and seedability is 0.96 for seeded clouds. For the unseeded clouds, the correlation between seeding effect and seedability is −0.42 which is not significant even at the 40-percent level. The diagrams suggest, however, that the tops of the unseeded clouds were systematically overpredicted by the model. This was indeed the case. In fact, for unseeded clouds the average algebraic error (predicted minus observed tops) was +480 m, while the average absolute error was 528 m. Our visual observations during the field program suggested that the destructive effect of the aircraft penetrations prevented three of the control towers and at least two seeded towers from reaching as high as they would have otherwise. An example of a cloud tower torn up by the penetration of two aircraft is illustrated later in figure 14. Another problem regarding

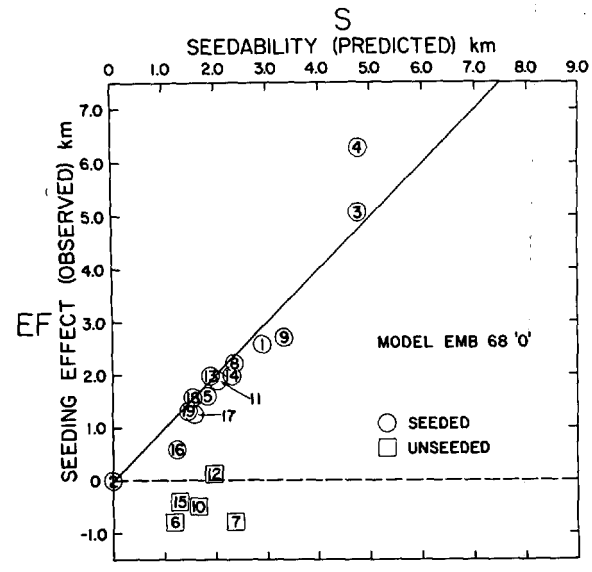

FIGURE 5.—Seedability versus seeding effect for model EMB 68 O.

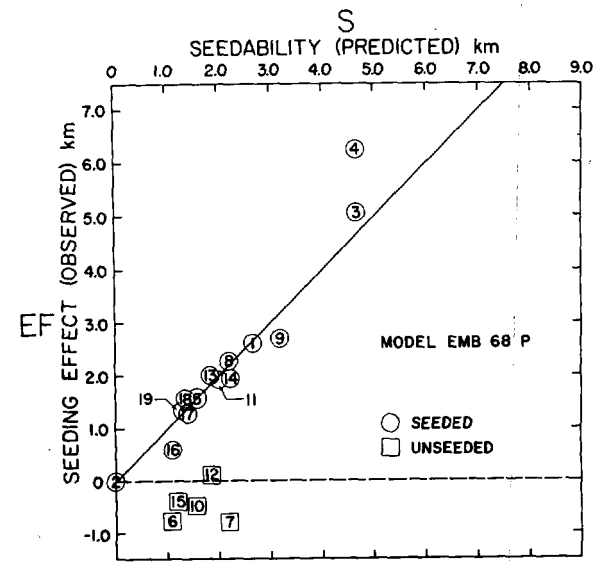

FIGURE 6.—Seedability versus seeding effect for model EMB 68 P.

TABLE 4.—*Precipitation comparisons*

Date	Cloud	K		O		P		Meas. ΔR (acre-ft)
		Δr (g kg^{-1})	ΔP	Δr (g kg^{-1})	ΔP	Δr (g kg^{-1})	ΔP	
May 15	1	−3.01	1.53	−0.97	1.53	0.10	1.47	94.5
16	2	−.05	.17	−.02	.23	.04	.24	5.1
	3	1.40	3.06	3.03	3.08	3.79	2.95	823.9
	4	1.40	3.06	3.03	3.08	3.79	2.95	200.8
19	5	−1.77	2.09	.17	2.20	.93	2.01	224.5
20	8	−2.28	2.00	−.46	2.11	.50	1.96	70.8
21	9	−2.16	2.06	−.02	2.10	1.19	1.99	no control
26	11	−1.75	1.93	−.14	1.97	.83	1.87	merger
27	13	−2.10	1.76	−.20	1.81	.75	1.71	70.5
28	14	−.57	2.18	.98	2.25	1.56	2.09	.8
30	16	−2.33	1.41	−.77	1.52	−.07	1.38	−105.2
	17	−3.08	1.50	−1.23	1.60	−.28	1.47	88.1
	18	−3.08	1.50	−1.23	1.60	−.28	1.47	−198.6
June 1	19	−1.49	1.66	.23	1.88	.79	1.72	data missing

the control clouds is seen on the diagrams, namely none had a seedability much exceeding 2 km. Unfortunately, on days of high seedability the randomization procedure chose no control clouds. This problem did not occur in 1965 and will be partially prevented in the 1970 experiment by randomization in pairs.

The relative accuracy of the models in predicting seeded heights differs little between K, O, and P. The average absolute height errors are respectively 333, 341, and 291 m. The superiority of the model P becomes more pronounced when rainfall and cloud physics are considered and compared with observations. Table 4 compares precipitation production and fallout between the three models and with radar measurements (Woodley 1970*a*). As explained in section 3, the fallout of precipitation from the rising tower in each interval is summed in one column of the computer printout. The final sum of fallout achieved when the tower reaches its maximum height is presented in figures 8, 10–12, 15–18, 20–21, 23, 25, and 28 as "seeded fallout" and "unseeded fallout," respectively. The difference between these two quantities appears as Δr in table 4. Δr is thus only the difference in fallout from the rising towers and not necessarily the rainfall difference at cloud base, although there should be a relation, as we shall see. ΔP is the total precipitation production of the rising tower, namely the summed fallout plus the precipitation content still contained in the tower at its peak height. The column labeled "Meas. ΔR" is the difference in radar-measured precipitation between seeded and control clouds for the first 40 min following the seeding run. On days when a randomly selected control cloud was available, it was used for this calculation. Where no randomly selected control was available, a radar control was used. No control cloud whatsoever existed on May 21. On May 26, the seeded cloud merged with a neighboring cloud by 10 min after seeding, and its water production could not be calculated. On June 1, the aircraft were forced to work outside the 100-n.mi. range of the University of Miami radar, and hence no radar measurements were possible.

On examining table 4, we immediately see that models K and O largely give precipitation decreases following seeding. In K, fallout from seeded clouds is decreased relative to unseeded clouds in 86 percent of the cases or in all but two cases, while with model O, the fallout was decreased in 64 percent of the seeded clouds. This result appears unrealistic in view of the observed increases from seeding. The reason for this outcome in the models stems from the reduced terminal velocities of ice particles in models K and O. The terminal velocities of ice were reduced for the purpose of loading the tower, thereby reducing its vertical momentum and preventing overprediction of top heights. Of course, it might be argued that the main reason that seeding increased precipitation was by producing a multitowered cloud where the precipitation from the first, actually seeded tower was in fact reduced. That this is not the case is demonstrated by a calculation of the correlation between the measured precipitation in the interval 0–10 min following seeding with the total measured precipitation in the interval 0–40 min following seeding. The correlation is 0.87, significant to the 0.5-percent level. Furthermore, the measured precipitation in the interval 0–10 min averages 27 percent of the total precipitation in the interval 0–40 min for both seeded and control clouds. This means that the first tower of the cloud gives both an amount proportional to and an appreciable fraction of the seeded cloud's total rainfall increase and that the model, which treats the first tower, should show precipitation increases that can somehow be related to an appreciable fraction of the measured rainfall.[3] A rough calculation readily shows that the Δr's in table 4 are numerically far smaller than the observed rainfall differences between seeded and control clouds in the last column of the table. For example, consider cloud 3 on May 16, with $\Delta r=3.79$ g kg^{-1} (for model P). With a cloud tower radius of 1000 m and a mean air density of about 0.5×10^{-3} g cm^{-3}, we have

$$\text{mass water}=\frac{4}{3}\pi\rho R^3\cdot\Delta r=4\times0.5\times10^{-3}\times10^{15}\times3.79\times10^{-3}$$

$$=7.6\times10^{9}\text{ g}$$

$$=6\text{ acre-ft}$$

compared to the observed difference of 823.9 acre-ft. We resolve this discrepancy with a precipitation growth model in section 7.

We note in table 4 that model P gives rainfall increases from seeding for all cases except the clouds on May 30, where decreases were actually observed in two out of three seeded clouds. Also, the May 16 predicted increases are the largest, in correspondence with the measurements. Model P permits the ice terminal velocities to be 70 percent of those of water particles of equivalent mass, as meas-

[3] It may seem inplausible to some readers that the seeding can affect the radar-measured rainfall at cloud base level as early as 10 min following seeding. A calculation demonstrating that this can and does happen has been published elsewhere (Simpson 1970).

ured by Braham (1964), and at the same time does not overpredict the cloud tops for two reasons. The first reason is the change in ice particle spectrum achieved by raising n_0 one order of magnitude to conform with figure 3. The higher n_0 means proportionally more small ice particles and hence reduced fallout. The combined and somewhat compensating changes in n_0 and terminal velocity lead to slightly greater fallouts and reduced retained precipitation in model P relative to K and O. The other factor reducing overprediction of top heights in P is that only 60 percent of the water at −4°C is frozen in this model, allowing for the higher observed amounts of ice in the pre-seeding penetrations.

Table 5 shows some important correlations between predictions and measured rainfall for all three models; and the significance tests have been made using one-sided t tests, since the advance prediction was made that the correlation should be positive. The first two rows in the table correlate physical predictions of the model with the measured difference between seeded and control precipitation, while the last two rows correlate the dynamic predictor seedability (S) with measured precipitation. The quantity ΔW is the water produced in the 0- to 40-min period after seeding, relative to the water produced in the interval 10 min before seeding.

First, we see that all correlations are positive and significant. This means that the model has considerable skill in predicting the relative amounts of rainfall to be gained from seeding. Then we note that all models are about equally good in relating seedability to rainfall increase. This is clearly because the seedability prediction varied little between models; the reason is that the dynamics of the clouds are not highly sensitive to the details of the microphysics. This statement is equally applicable to model A (table 1), the version used in real time in advance of each operation; the seedabilities computed with model A differed little from those of K, O, and P. However, when we compare on the basis of computed precipitation fallout differences (table 4), model P is clearly superior to the others. This is gratifying since P is based on a much closer fit of the ice parameters to observations.

Last, we can show that the important correlations would be much higher if we could correct for one serious error in the radar measurement of precipitation. In table 3, we note that the predicted Δr's of clouds 3 and 4 of May 16 are equal, while the measured ΔR for cloud 3 is listed as exceeding four times that of cloud 4. Simpson and Woodley (1969) noted that cloud 4 was in the blind cone of the University of Miami radar, produced by the interference of the library building. They deduced from aircraft penetrations and other evidence that the echo intensity and rain production of cloud 4 should have been at least equal to that of cloud 3. With this correction in the rainfall of cloud 4, the results with model P come out as follows: *The correlation between seedability and rainfall increase is 0.87 and the correlation between predicted and measured rainfall increase is 0.91,* both significant to better than 0.5 percent.

This important result provides a possible way to predict the actual amounts of rainfall increases from seeding in advance, from a prediction of seedability. Seedability is a dynamic variable that our several experiments (see also Simpson et al. 1967) have shown predicts actual cloud growth to good accuracy. Figure 7 shows a plot of the observed ΔR in acre-feet versus predicted seedability in kilometers. The equation

$$\Delta R = -286 + 211\ S \qquad (10)$$

is the equation of the best fit straight line to the points in

TABLE 5.—*Correlations between predictions and measured rainfall for 1968 seeded clouds*

	K		O		P	
	Correlation	Significance (%)	Correlation	Significance (%)	Correlation	Significance (%)
Δr, ΔR	0.63	<2½	0.73	~½	0.75	<½
ΔP, ΔR	.63	<2½	.63	<2½	.65	<2½
S, ΔR	.70	<1	.70	<1	.71	<1
S, ΔW	.67	<1	.67	<1	.67	<1

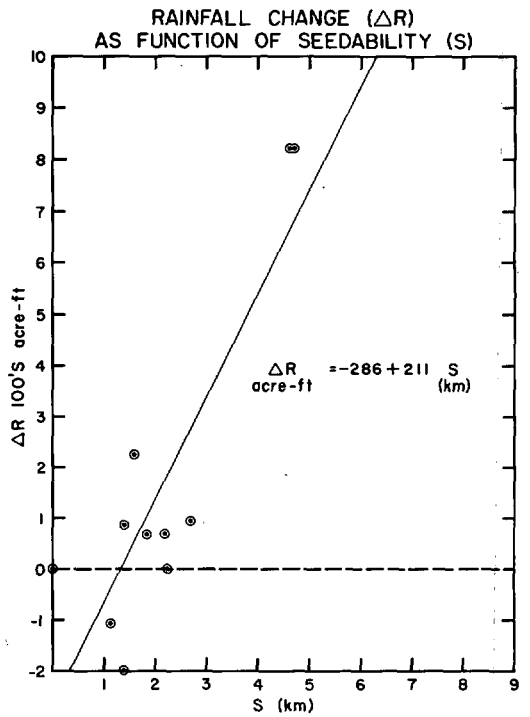

FIGURE 7.—Radar-measured precipitation change (ΔR) in the seeded clouds of 1968 plotted versus the model-computed seedability for the same cloud. ΔR is the precipitation difference (measured at cloud base) between the seeded and the control cloud. The equation on the right is that of the straight line that best fits the data points.

TABLE 6.—*Predicted versus observed cloud tops for 1968 experiment model P used for seeded clouds*

Cloud	Date	Observed maximum top (km, abs. alt.)	Predicted unseeded top (km)	Predicted seeded top (km)
①	May 15	13.46	10.88	13.58
②	16	6.10	6.05	6.10
③	16	12.90	7.80	12.45 (13.00)*
④	16	14.10	7.80	12.45 (14.30)*
⑤	19	11.12	9.48	11.08
⑥	19	7.02	7.78	8.83
⑦	20	7.42	8.23	10.43
⑧	20	11.69	9.43	11.63
⑨	21	12.83	10.12	13.32
⑩	26	6.82	7.37	8.92
⑪	26	11.71	9.77	11.77
⑫	27	10.12	10.00	11.85
⑬	27	12.00	10.00	11.85
⑭	28	10.41	8.41	10.66
⑮	30	9.7	10.10	11.29
⑯	30	10.61	9.96	11.11
⑰	30	11.92	10.63	12.08
⑱	30	12.20	10.63	12.08
⑲	June 1	9.99	8.61	9.96

*Top using expanding radius measured by photogrammetry (Simpson and Woodley 1969). (See also figs. 10 and 11.)

figure 7 found by the method of least squares. The variance of ΔR is reduced by 0.76 by this relation.

We might expect the rainfall increase to be smaller, the greater the unseeded cloud top. When this dependence is introduced, the best fit linear equation for ΔR becomes

$$\Delta R = 416 + 200\ S - 74\ P_u \qquad (11)$$

where P_u is the predicted unseeded top in kilometers (see table 6). The introduction of the second variable dependence reduces the variance by an additional 10 percent.

Clearly, there are too few data points at present for these results to be applied confidently to practical modification. In future experiments, we plan to investigate whether one relationship of this type can be constructed for South Florida, or whether perhaps different curves are needed for different synoptic situations. Meanwhile, it is important to note that, when seedabilities are less than about 1 km, rather sizable decreases in precipitation follow massive seeding. This point is clarified further in section 8.

6. MODEL P RESULTS FOR INDIVIDUAL CLOUDS

Table 6 gives the model-predicted[4] and the observed cloud tops for each GO cloud in the 1968 experiment. The observed tops were measured by aircraft and/or photogrammetry. Simpson et al. (1970*b*) presented these measurements earlier in units of pressure altitude. In table 6, pressure altitude has been converted to absolute altitude using the U.S. Standard Atmosphere and the soundings of table 3. In the height region where cloud tops occur, the absolute altitude is very roughly 1,000 ft higher than the pressure altitude.

Figures 8, 10–12, 15–18, 20–21, 23, 25, and 28 show plots of the individual model results for each GO cloud. Observed tops (with radius and cloud base subtracted) have been entered as a horizontal line on each diagram. On examining these figures, we see that the 1968 experiment was in some ways not as good an experiment in cloud dynamics as was the 1965 experiment (Simpson et al. 1967, appendix table). The randomization in 1968 gave only five control clouds. Of these five, only two (May 27 and 30) had the same environment and the same or nearly the same radius as a seeded cloud and hence formed a perfect pair. The remaining three had smaller radii than the corresponding seeded clouds, while two of these (May 19 and 26) grew in much less favorable environments. Randomization in pairs will help but not completely solve this type of problem in future experiments.

The 1965 experiment, however, definitively established the relation between seeding and cloud growth. The main advance resulting from the 1968 experiment lies in relating the microphysics and rainfall to the dynamic effects of seeding.

We now discuss briefly the model results and observations for each cloud.

MAY 15 (FIGS. 8 AND 9)

Cloud 1 was unfortunately seeded when its top had already attained 30,000-ft pressure altitude, or about 8.8 km above cloud base. Figure 8 shows that the unseeded cloud should have topped out just above this level. Figure 9 shows "before and after" photographs of cloud 1. The wind shear was very weakly from the north so that the cloud grew almost vertically. The cloud's life history consisted essentially of the growth, spreading, and decay of the single, very wide tower. The seedability was 2.7 km, and the predicted and observed seeded tops agreed closely.

Table 4 shows that of the positive predicted Δr's, that for cloud 1 is the second smallest due to the great height predicted for the unseeded tower. The only control cloud on May 15 was a radar control. The difference between seeded and control precipitation was 94.5 acre-ft, one of the smaller than average increases. Cloud 1, moreover, was one of the few seeded clouds in 1968 for which ΔW was negative for the most of the 40-min period following seeding. ΔW is the rain falling in a 10-min interval minus the rain falling 10 min before seeding. This result probably occurred because the natural top was very high and had rained heavily before seeding.

Foil sampler records were not available for this day, and the individual cloud penetrations showed no especially interesting features.

MAY 16 (FIGS. 10 AND 11)

All three GO clouds on May 16 were seeded, and the only control is a radar control. The three seeded clouds

[4] The cloud radius and height of cloud base have been added to each model-predicted top, since the model calculates the height of the tower center above cloud base.

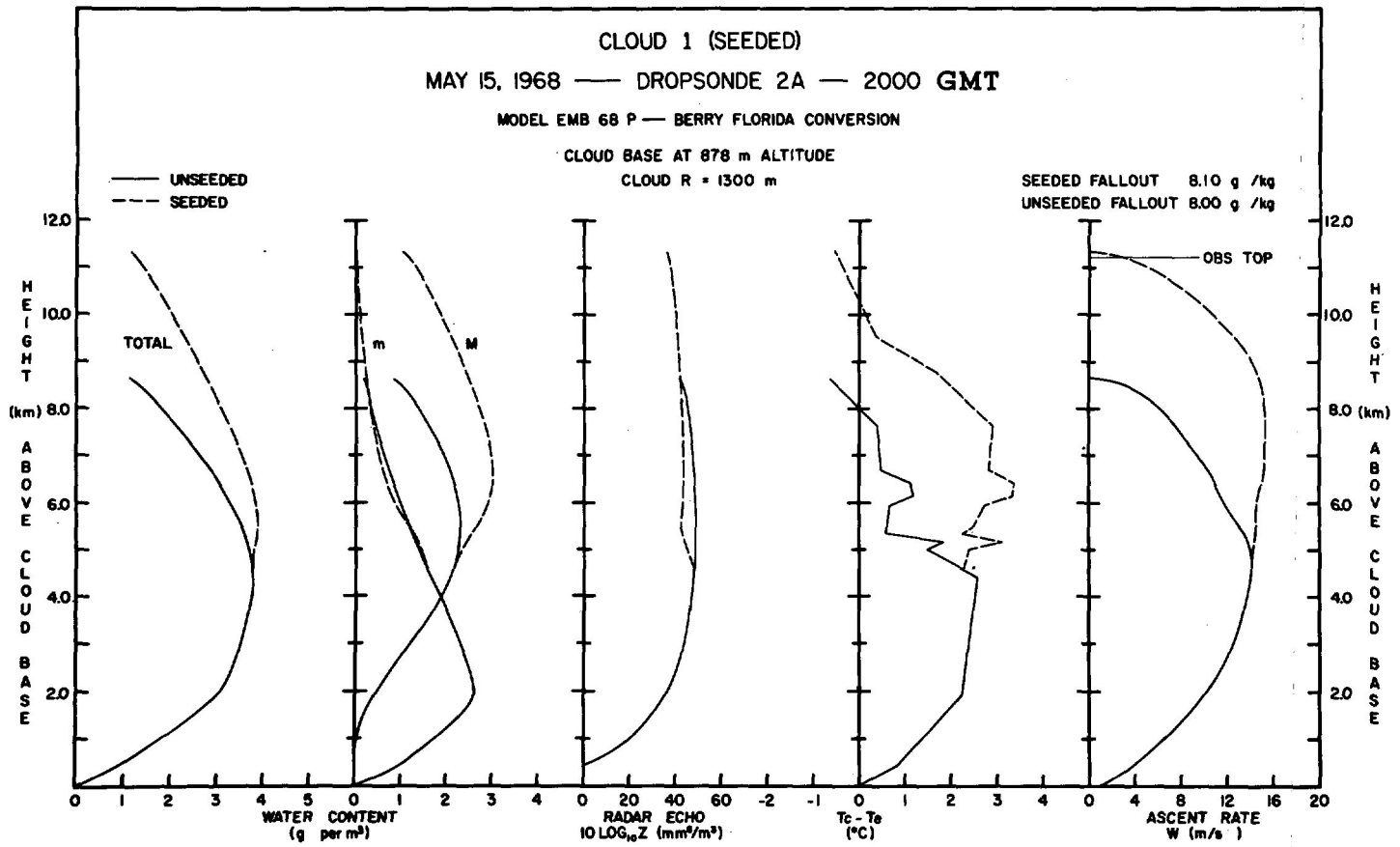

FIGURE 8.—Results of model calculation for cloud 1 on May 15, 1968. Properties of the rising tower center as it rises are plotted against height above cloud base (ordinate). On the left is the total water content (in g m^{-3}). Next is the water content broken down into cloud water, m, and precipitation water, M. The middle curve is radar echo in units of decibels or 10 $\log_{10} Z$ (where Z is in $mm^6 m^{-3}$). The second-from-right curve is within-cloud temperature excess, and the right-hand curve is the rise rate of the tower. The observed top has been modified by subtracting the tower radius and cloud base height because the model predicts the height of the tower center above the cloud base.

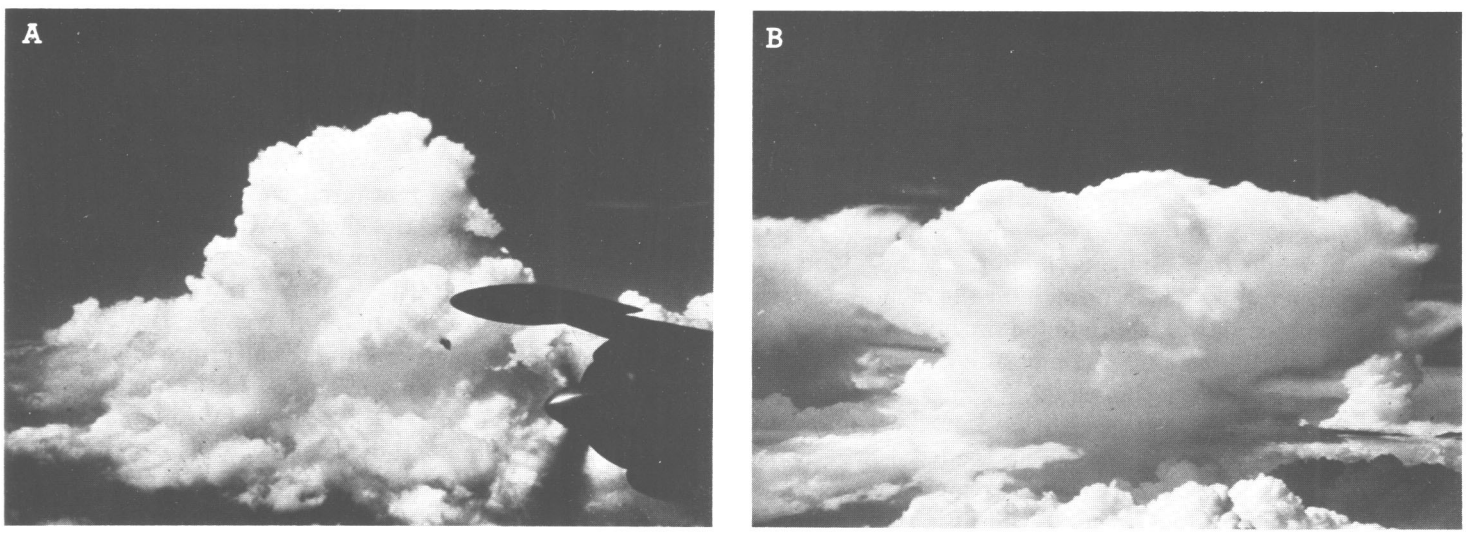

FIGURE 9.—Photograph of cloud 1 (seeded) on May 15, 1968 (by Mr. Robert Ruskin, Naval Research Laboratory); (A) the cloud 8 min before seeding at the time of the first monitoring pass and (B) the cloud 30 min after seeding with full cumulonimbus stature.

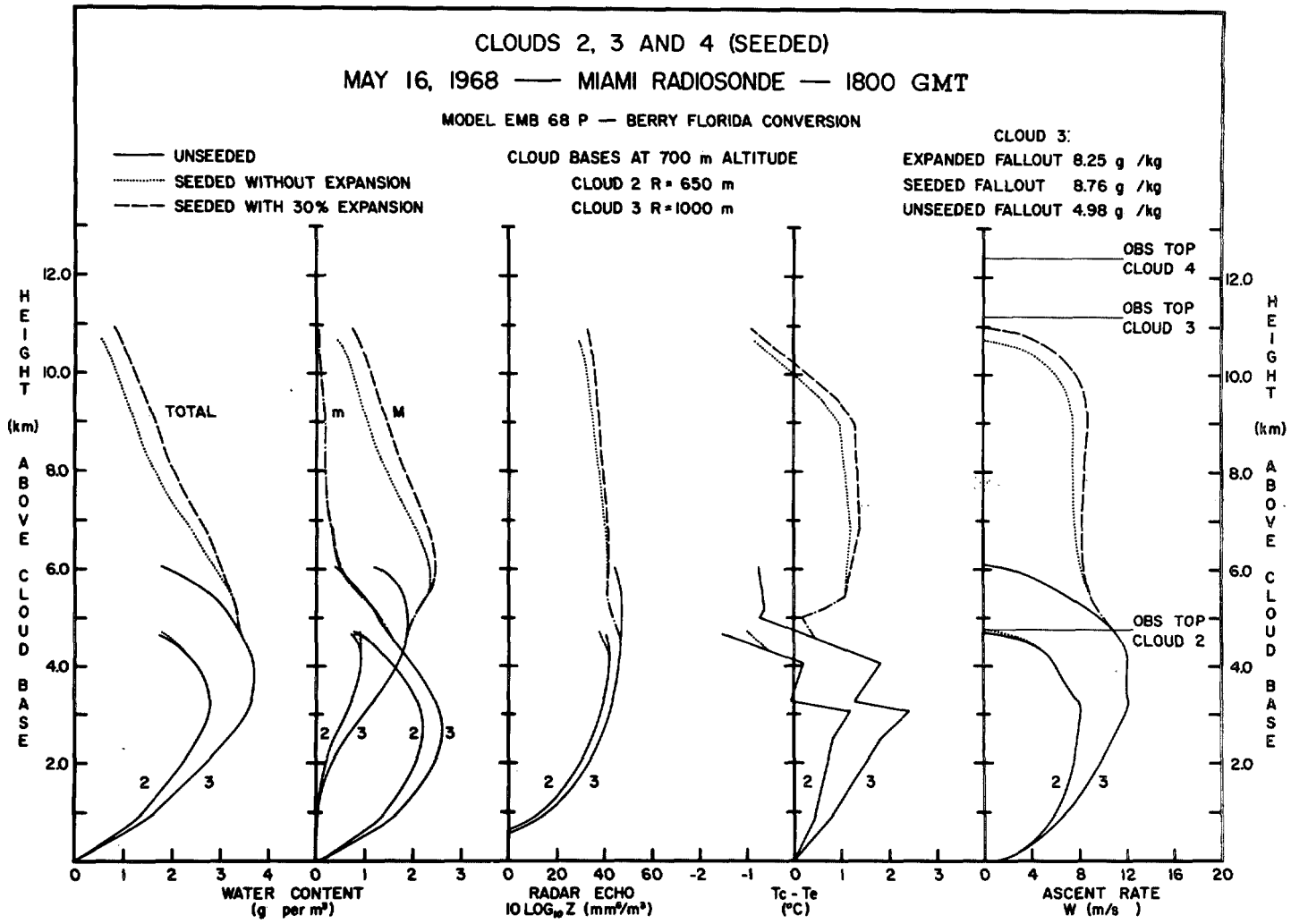

FIGURE 10.—Model results for clouds 2, 3, and 4 on May 16, 1968. Cloud 3 has been considered without (dotted) and with (dashed) the measured 30-percent expansion. Cloud 4 is considered only without expansion (dotted) here (see also fig.11).

have been described in detail elsewhere (Simpson and Woodley 1969) and will only be briefly summarized here.

Cloud 2 was the only cloud in the 1968 series that failed to grow following seeding. The measured tower radius was 650 m, the narrowest of the program; and the predicted seedability was only 0.05 km or virtually zero. Figure 10 shows that model and observed results are in fine agreement. The DC–6's pre-seeding run at 19,000-ft pressure altitude passed over the top of the cloud. At that time, the top was descending and the cloud body was beginning to dissipate. The predicted precipitation increase in table 4 is negligible as is the measured excess of seeded over control rainfall for this cloud.

Cloud 3 grew explosively, with the initial seeded tower participating in the explosion. The seeded tower had a measured radius of 1000 m at seeding, expanding gradually to 1300 m during the following 7½ min it took to achieve its maximum growth. Near the end of its vertical growth, it merged with another tower of approximately the same size. The 1000-m radius has been used in all statistical calculations to be consistent with the method of radius determination for the other clouds. The 30-percent expansion to 1300 m is included in the calculation shown by the dashed lines in figure 10, which gives better agreement with the measured cloud top.

The pre-seeding DC–6 run passed through the core of the actively rising (later seeded) tower on cloud 3; and a detailed comparison of measured water contents, precipitation spectra, and radar echoes with model results was highly satisfactory (Simpson and Woodley 1969). With model P, we get nearly the same rise rates of the tower as we did with model K in the earlier work. Both compare very closely with photogrammetrically measured values. Table 4 shows that cloud 3 was both predicted and measured to have the greatest rainfall increases from seeding of any cloud studied in 1968. Its precipitation growth processes are examined further in section 7. Cloud 3 put up four or five major towers in its 145-min lifetime, or roughly one each 30 min.

Cloud 4 appears both in figures 10 and 11. It appears in figure 10 because the measured radius on the first DC–6 box following seeding was 1000 m, which was used in

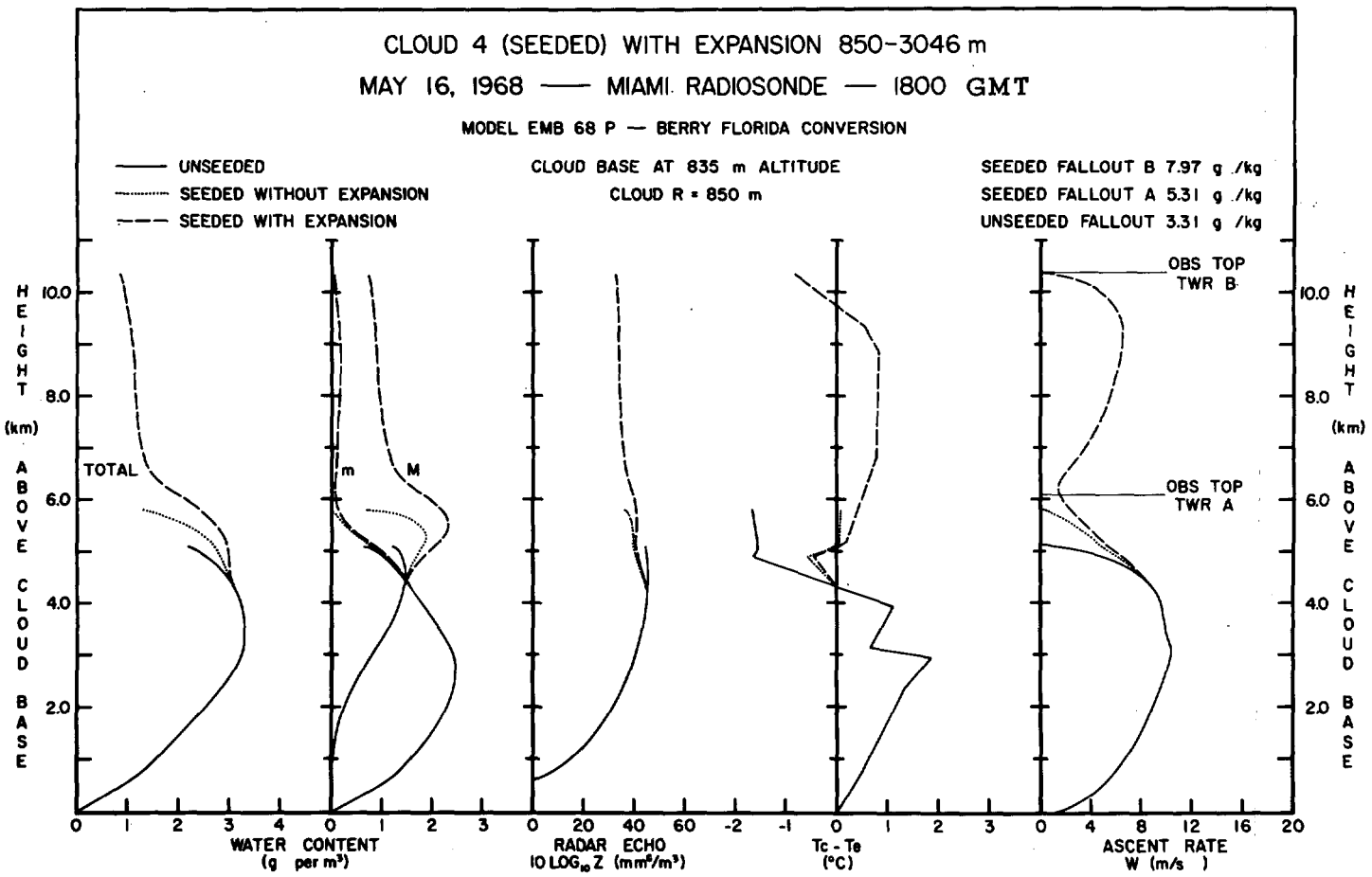

FIGURE 11.—Model results for cloud 4 on May 16, 1968, considering the measured expansion of tower B (dashed). Tower A that had a non-expanding radius of 850 m is shown by the dotted seeded curve.

all statistical calculations. Figure 10 shows that a rather poor agreement between predicted and observed seeded tops results with this radius, which, however, was used in construction of figures 4–6. The photogrammetry, which consisted of measurements of heights and radii with time, showed that the actual growth of cloud 4 was complicated. This cloud showed a "hesitation growth" because two towers were seeded in very different stages of their life cycles. Tower A, penetrated before seeding by the DC-6, was near its maximum unseeded top (about 6 km) and in a late stage of its life cycle. Tower B (unpenetrated before seeding) was much lower, very young, and still embedded partially in surrounding cloud matter. Both measured 850 m in radius before seeding. Following seeding, tower A grew upward slightly without expansion and dissipated, while tower B was able to expand its radius nearly fourfold and thereby grow up above 14 km, where it was soon followed by still another expanding tower, C.

Figure 11 shows that the model treats the actual complex situation very well, with the reservation that it cannot explain or predict the expansion and can only assume it as measured. We see that the unexpanded 850-m tower is predicted to die with little growth, while the expanded tower grows easily to the height observed with tower B.

Clearly, the seeding did something more drastic and more complex to cloud 4 than just enhance the vertical growth of an already formed tower. It somehow permitted tower B to expand drastically in the horizontal, thus permitting its vertical growth. Horizontal expansion is invariably a key part of explosive cloud growth and usually follows the vertical growth of the first seeded tower (Malkus and Simpson 1964). Here, the horizontal phase of the explosion began with the first rising tower. We hypothesized that this was enabled because tower B was partially surrounded by moist cloud matter when seeded, rather than completely isolated in the clear, as was tower A.

The computed rise rates for tower B using model P agree much better with measured rise rates than did those computed earlier with model K. In the interval 6–7 km above cloud base, the computed rise rate is 2.4 m s^{-1} compared to a measured value of 4.5 m s^{-1}. In the interval 9–10 km above cloud base, the model computed 6 m s^{-1} while 7.5 m s^{-1} was measured. In the whole 5700-m rise above the seeding level, the predicted average rise rate was 4.6 m s^{-1} while the measured value was 6.8 m s^{-1}.

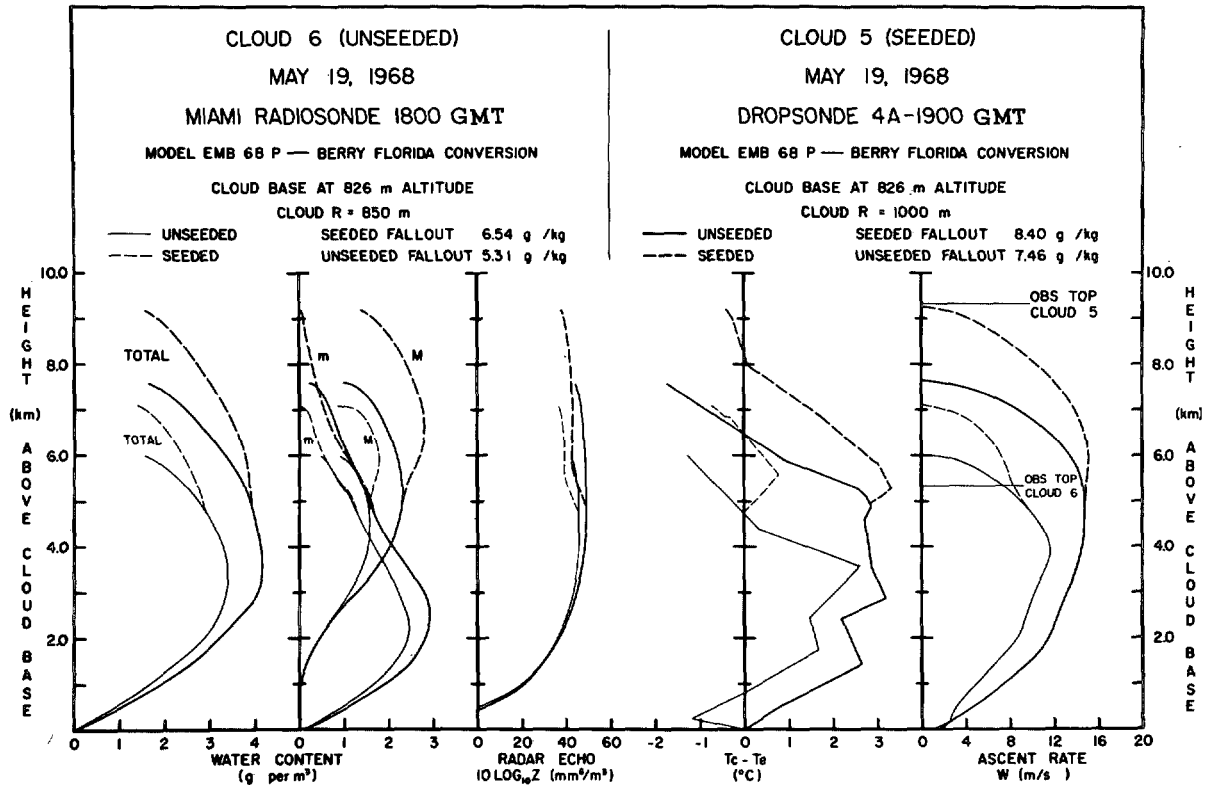

FIGURE 12.—Model results for cloud 5 (heavy lines) and cloud 6 (light lines) on May 19, 1968.

Using figure 10, we calculate a Δr of 3.79 g kg^{-1} for cloud 4, while figure 11 gives 4.66 g kg^{-1}, the largest predicted rainfall increase for the whole program. As we mentioned earlier, the value of ΔR of 200.9 in table 4 for this cloud was shown to be erroneously low; the correct value of ΔR is probably 800–1000 acre-ft.

MAY 19 (FIGS. 12, 13, AND 14)

On May 19, both a seeded and a control cloud were obtained by the sealed envelope procedure. Unfortunately, however, the aircraft-sampled environment of the control cloud was considerably drier and thus less favorable for cumuli than was the environment of the seeded cloud. Hence the measured difference in their tops is not representative of growth that could have been achieved by seeding in any one location on that day.

Although *cloud 5* (seeded) was studied 2 hr earlier than *cloud 6* (control), the Miami 1800 GMT radiosonde most closely resembled the environment of cloud 6 (penetrated first at 1953 GMT) while Air Force dropsonde 4 at 1900 GMT best represented the environment of cloud 5, seeded at 1755 GMT. A detailed study of the dropsondes and radiosondes in the South Florida area on that day showed rather small time variations and rather large space variations, the latter often occurring in distances as small as 10 mi.

Cloud 5 has been studied in detail by Woodley (1970*b*). Before seeding, it consisted of two towers lined up north-south, the lower and younger tower on the south. The DC-6's pre-seeding pass penetrated the more northerly

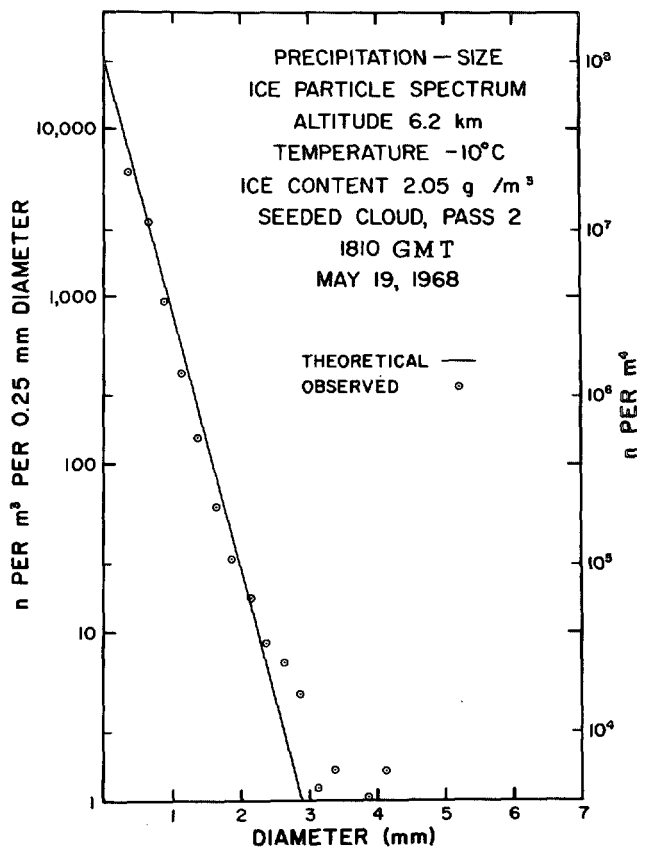

FIGURE 13.—Precipitation-size ice particle spectrum measured by the foil sampler for cloud 5 on May 19, 1968. Measurement was made on an aircraft pass about 15 min after seeding, about 5 km below the cloud top.

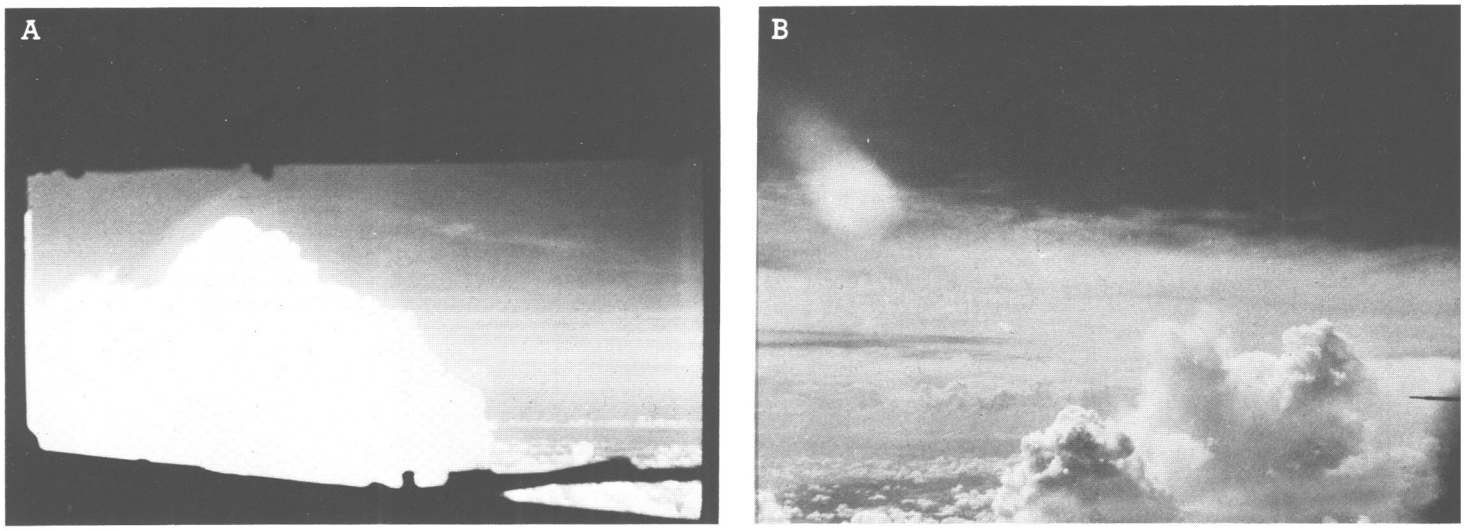

FIGURE 14.—Photographs of cloud 6 (control) on May 19, 1968; (A) cloud as the DC-6 approaches the first penetration, 4 min prior to the "seeding" run and (B) the same cloud immediately after penetration by the DC-6 and WC-121 aircraft; note the apparent destruction of the tower by the aircraft.

tower, flying from west to east. The foil sampler showed that 87 percent of the precipitation particles were glaciated on this pass, with an ice particle concentration of 9 per liter. The high degree of glaciation plus the fact that the hot wire showed only 0.4 g m^{-3} cloud water indicates an aging tower that in fact dissipated before or during the first seeding run. The latter was made from south to north through both towers. Photogrammetry shows clearly that both towers ($R \sim 1000$ m) had stopped growing at about 8.8 km before seeding and that the old north tower was actually descending. Following seeding, the southerly tower began rising suddenly at about 12 m s^{-1} without much expansion, then merged with a new tower to its north that rose from the middle of the old cloud body. As seen in figure 12, the observed and model rise rate for the north tower after seeding agree fairly well. The observations suggest that the predicted unseeded top of cloud 5 of 9.48 km (table 6 and fig. 12) is an overprediction by about 0.7 km. Further evidence is that a seedability of 2.3 km would from figure 7 give a ΔR very close to the observed value of 224.5 acre-ft. With the computed seedability of 1.6 km, the point for cloud 5 on this graph lies way above and to the left of the straight line.

The reason that the model overpredicts the unseeded growth of cloud 5 is readily found in the sounding used. Dropsonde 4 had an abnormally wet 70-mb layer near 500 mb, not present on the other soundings of that day, probably due to the instrument's passing through the cloud. This unrepresentative wet layer would have given an artificial "boost" to the model clouds, particularly the unseeded ones which should have otherwise begun decelerating there.

DC-6 pass 2 through cloud 5 was made beneath the main actively growing tower, about 15 min after the first seeding. By this time, the cloud had achieved more than 11 km with full cumulonimbus stature; and its top was nearly 5 km above the aircraft. Nevertheless, these measurements offer some interesting comparisons with model calculations. Figure 13 shows the ice particle spectrum measured by the foil sampler compared with the straight line (Marshall-Palmer spectrum) used in the model, with $n_0 = 10^8$ m^{-4}. The agreement is excellent except for the observed presence of large ice particles with diameters above 3 mm, where the theoretical concentration falls below 1/m^3. By this time, these particles could easily have fallen down to 6.2 km from higher levels in the cloud. Actually, some 11-mm ice particles were measured in a concentration of 1/10 m^3, with 3 percent of the IWC (ice water content) in this size. Of the total IWC, 24 percent was in particles greater than 3 mm in diameter. The average ice particle concentration throughout the run was 9 per liter, the same as in the pre-seeding run in the old northern tower. The precipitation content of the cloud was now 89-percent glaciated. The Johnson-Williams hot wire (Neel 1955) had two tiny peaks of 0.2 g m^{-3}, indicating either that there were negligible amounts of cloud-sized water particles or that these particles were frozen.

The total water content in precipitation sizes from the foil was 2.3 g m^{-3} while the Levine (1965) instrument measured 1.8 g m^{-3} total water content. This and other evidence indicates that the Levine instrument is responding rather well in measuring ice. What is not clearly specified is the water content in cloud-sized particles. For the actively rising tower at this level, the model predicts 2.4 g m^{-3} in precipitation (M) and 1.5 g m^{-3} in cloud water (m).

Finally, we may compare volume median precipitation particle sizes and radar echo between model and observed values. The model gives the volume median precipitation

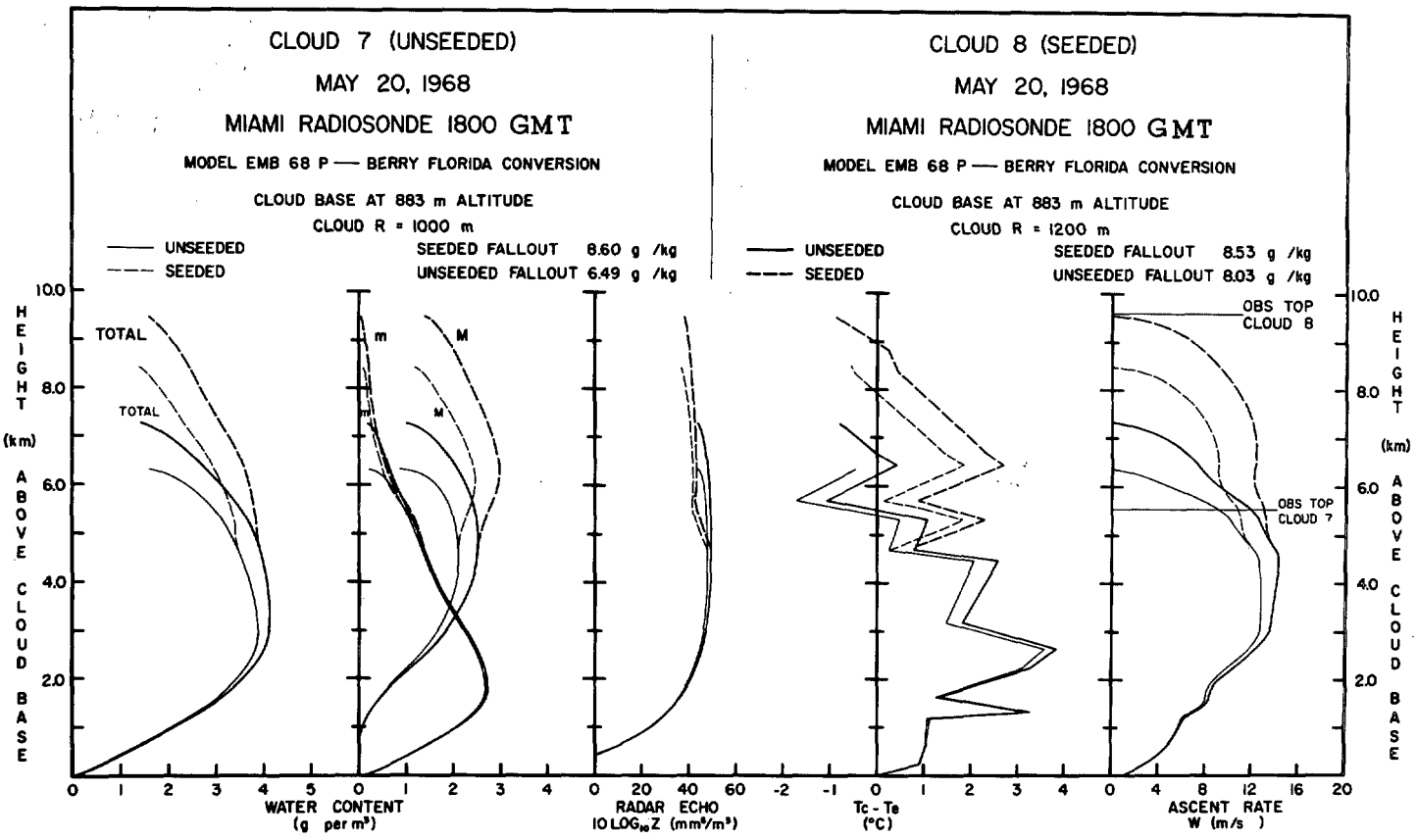

FIGURE 15.—Model results for cloud 7 (light lines) and cloud 8 (heavy lines) on May 20, 1968.

particle size as 1.44 mm while the foil sampler gives 1.34 mm, a gratifying agreement under the circumstances. The radar reflectivity predicted by the model is 3.4×10^4 mm^6 m^{-3} while the value calculated from the foil spectrum is one order of magnitude higher, namely 3.5×10^5 mm^6 m^{-3}. The latter value was confirmed by the University of Miami 10-cm radar that showed a peak exceeding 2×10^5 mm^6 m^{-3} in this cloud at this time. At this stage of the cloud's development, this large discrepancy with the model is to be expected and is explained by the very large particles in figure 13.

Cloud 5 illustrates again the dependence of seeding effects upon the stage of a cloud tower in its life history. Here, there were two towers of roughly equal seedability, of which one was seeded in the dissipating stage and failed to grow, while the younger one grew explosively.

Cloud 6 (control) grew in the dry air on the southwest flank of a larger cloud complex. The tower that the DC–6 and seeder penetrated was almost surely destroyed by the aircraft, as shown by figure 14. Hence the predicted unseeded top exceeded that measured by photogrammetry (fig. 12). Several succeeding towers probably reached slightly higher but could not be measured.

MAY 20 (FIG. 15)

The seeded cloud and the control cloud on this day were almost a perfect pair, with identical environments and the same seedability (2.2 km each). The control cloud died without growth; and the seeded cloud grew to cumulonimbus stature, with the original seeded tower leading the explosion. The only flaw in the situation was that the control tower was a member of a 20-mile-long cloud line; and we therefore suspect that its measured precipitation exceeds what would have been obtained for an isolated cloud, due both to interaction effects that enhanced actual precipitation and to measurement problems. In table 4, we show a measured seeded versus control difference of 70.4 acre-ft; while in figure 7, a seedability of 2.2 km would give about 200 acre-ft, a more plausible value.

Cloud 7 was near the center of a line extending northeast-southwest and moving toward the southeast. Several towers were penetrated including the GO tower just in advance of the "seeding" run. These towers showed about 0.1 g m^{-3} precipitation, entirely frozen, and 2.0–2.5 g m^{-3} unfrozen cloud water as evidenced by the Johnson-Williams hot wire. A photographic study suggested that the aircraft penetrations may have caused the penetrated towers to dissipate sooner than those not penetrated, perhaps explaining why cloud 7 did not attain the predicted unseeded top in figure 15.

The GO tower in *cloud 8* was physically identical to the GO tower in cloud 7, with the pre-seeding penetration showing 0.1 g m^{-3} precipitation, all ice, and a Johnson-Williams reading of 2.2 g m^{-3}. After seeding, this tower

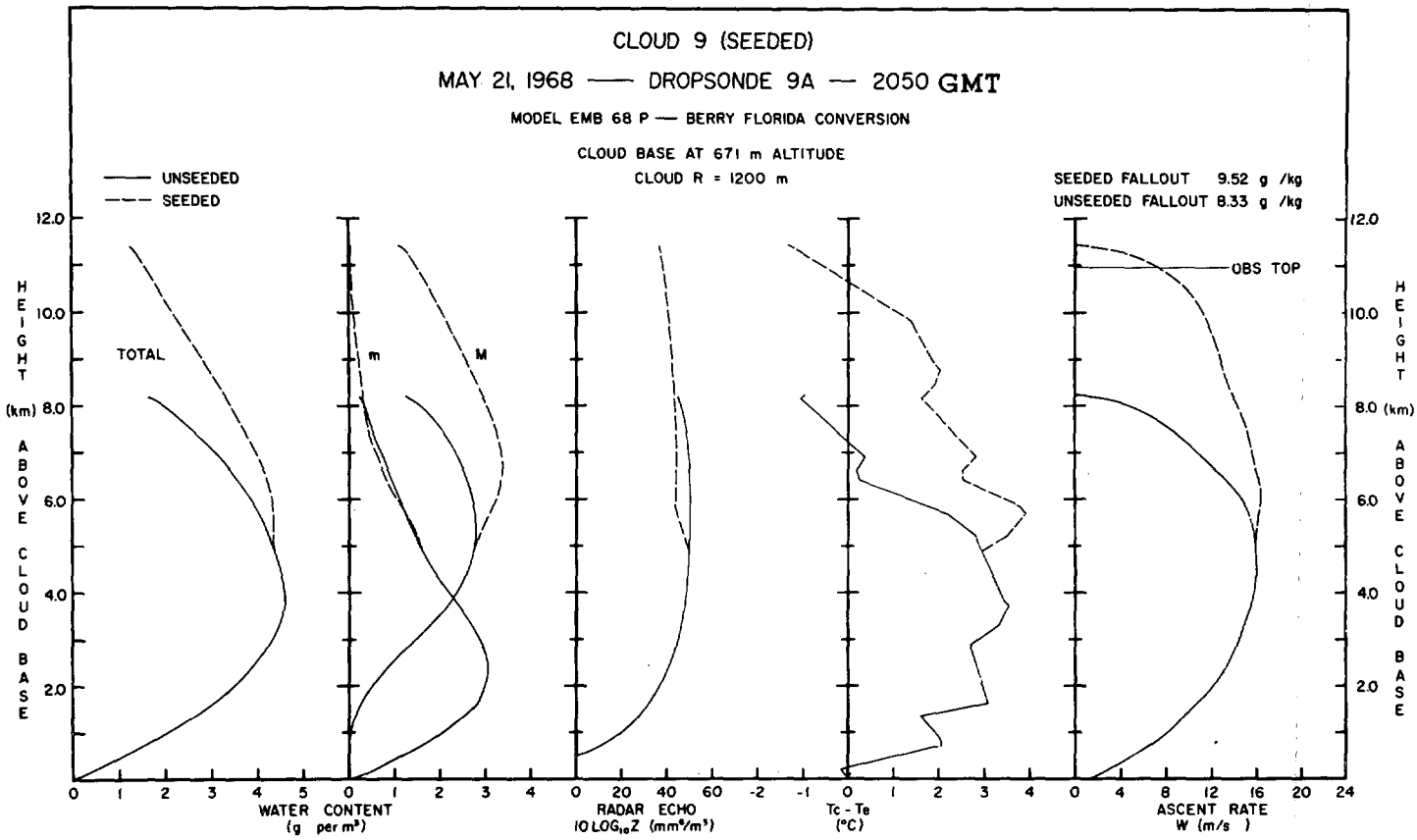

FIGURE 16.—Model results for cloud 9 on May 21, 1968.

grew above 10.0 km without much expansion; and the whole cloud underwent a classical version of explosive growth.

MAY 21 (FIG. 16)

On this day, the seeding operation had to be terminated due to the invasion of the experimental area by layers of cirrus and altostratus clouds. However, early in the day one GO cloud was obtained, which grew explosively following seeding. Predicted seedability was large (3.2 km), and the observed seeded top was in fair agreement with that predicted (fig. 16). Although no randomized or radar control clouds could be selected, there was a cloud penetrated prior to the seeder's arrival which had roughly the same horizontal dimension as the seeded cloud and topped out at about 8 km (by radar).

The pre-seeding penetration on *cloud 9* went through the center of the active tower and provides some valuable information concerning modeling that is shown in table 7. The model (unseeded) gives a total water content of 4.22 g m^{-3} of which 2.78 g m^{-3} is precipitation and 1.44 g m^{-3} is cloud water. The agreement is not bad, especially if we allow for a less-than-complete response of the Levine instrument to ice. The foil sampler showed that all the precipitation was frozen, with a median volume diameter of 1.35 mm. The median volume diameter from the model is 1.51 mm if the particles are ice and 2.02 mm if they are water. In this case, 44 percent of the cloud's water was in the form of frozen precipitation prior to seeding. This ratio was typical of numerous other pre-seeding runs studied. These were the figures used to specify that 60 percent of the total water at −4°C was to be frozen in the seeding subroutine of model P.

TABLE 7.—*Pre-seeding pass for cloud 9 on May 21, 1968*

Hydrometeor category	Amount (g m^{-3})	How determined
Total H_2O	3.3	Levine
Diameter <40 μm	1.0	Johnson-Williams
Diameter >375 μm	1.5	Foil (all ice)
Diameter between 40–375 μm	.8	By subtraction

MAY 26 (FIG. 17)

This was a poor day for the experiment for several reasons. Conditions were very disturbed (Fernandez-Partagas 1969), and several layers of cirrus and altostratus obscured cloud tops. The control cloud was 36 mi from Miami, which had very poor conditions for convection, while the seeded cloud was less than 30 mi from Key West in a much more favorable environment.

413-002 O—71——3

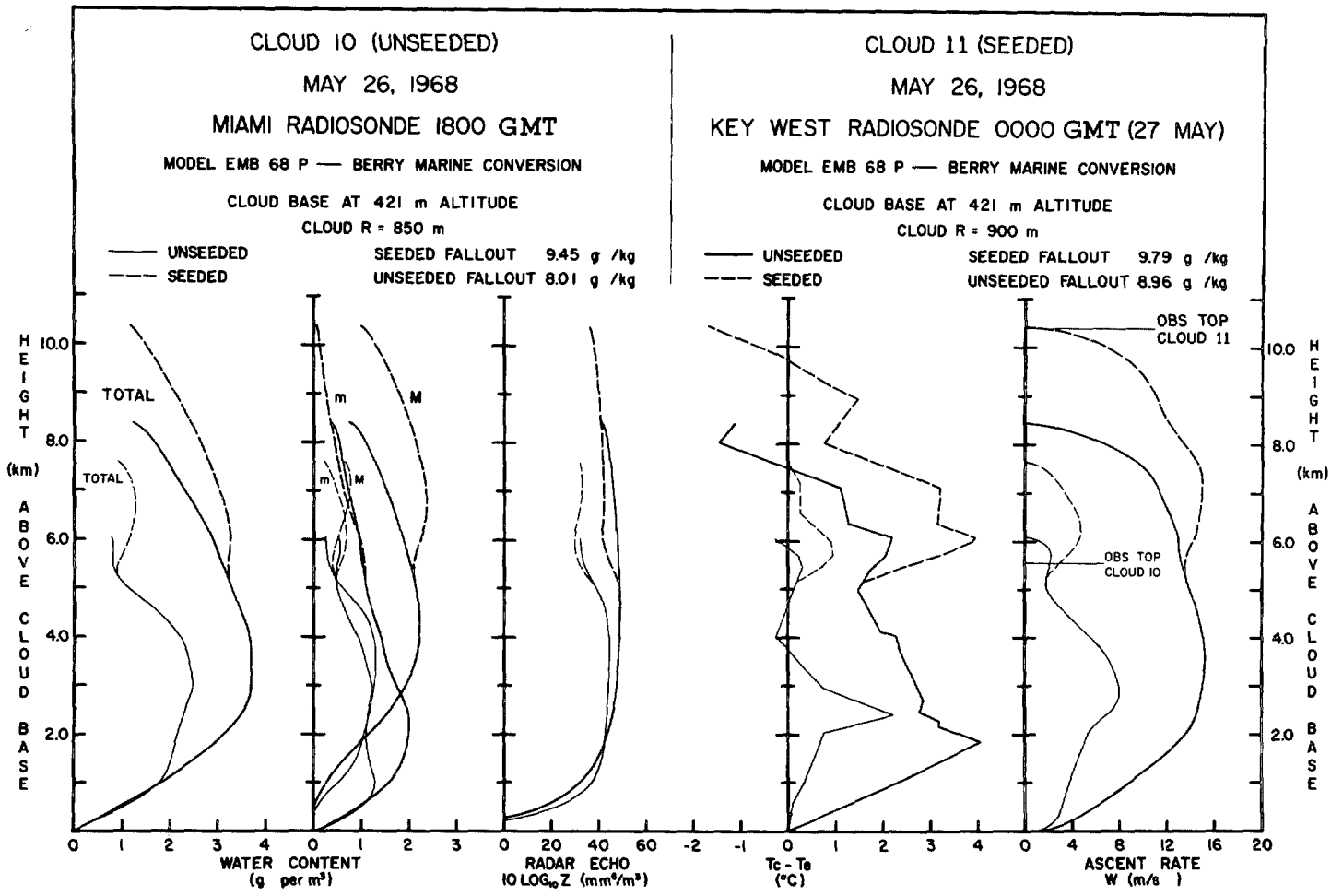

FIGURE 17.—Model results for cloud 10 (light lines) and cloud 11 (heavy lines) on May 26, 1968.

Figure 17 shows that the predicted unseeded top of the seeded cloud exceeds the predicted seeded top of the control cloud by nearly 1 km. Unfortunately, no seeded minus control cloud precipitation measurement could be made on this day either. The seeded cloud echo merged with neighboring echoes at 10 min after seeding. The control cloud had no echo at all, indicating insignificant precipitation from it.

Cloud 10 (control) was studied offshore in the vicinity of Miami at about 1738 GMT. Its top penetrated the altostratus into a stable layer above. The photographs indicate the aircraft effect may have caused its top to dissipate short of the predicted unseeded top height. The precipitation particles were all frozen at the time of the seeding pass. No information on cloud water is available since the Johnson-Williams was inoperative.

Cloud 11 was seeded less than 30 mi from Key West at 1823 GMT. Unfortunately, the Key West 1800 radiosonde was missing. Since all dropsondes were made north of cloud 10, the 0000 GMT Key West radiosonde for May 27 was used with this cloud with good results (fig. 17). Before seeding, all precipitation particles were frozen; and no information exists on the cloud water content. Following seeding, the tower grew explosively into the high overcast.

MAY 27 (FIGS. 18 AND 19)

On this day, the aircraft worked in the clear to the west of the disturbed region over the Florida Peninsula, selecting for study two marine clouds located in the Gulf of Mexico off the Florida west coast (fig. 1). This was the only occasion of a perfect seeded and control pair during the entire experiment. Both clouds grew in the same environment, had the same radius, and succeeded one another with less than a 1-hr interval. Predicted and observed tops were in near-perfect agreement for both seeded and control clouds (fig. 18). The seedability was, however, not large (1.85 km).

The vertical wind shear on this day was the third strongest of the experiment, and it was the only strong shear day with clear-enough skies for extended photographic studies of the GO clouds. The shear vector between 4,000–35,000 ft was 43 kt from the west-southwest. All clouds reaching to 30,000 ft or more developed extended anvils reaching tens of miles eastward.

Both seeded and control clouds underwent similar growth regimes, with thin weak bodies, strong slant, and long anvils (fig. 19). *Cloud 12* (control) only failed by 500 ft of being the highest control of the program. It was double-towered and after the "seeding" run became a per-

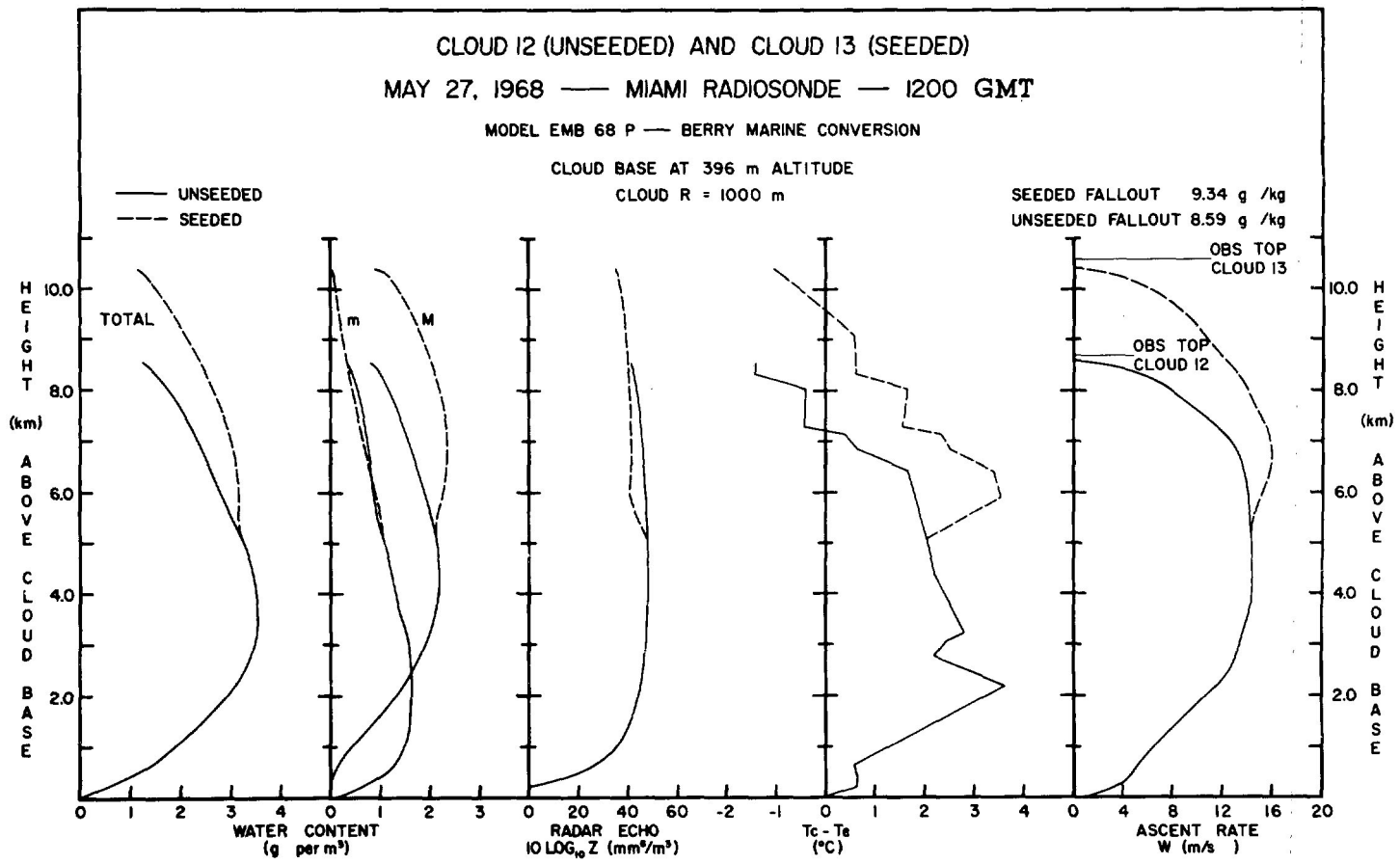

FIGURE 18.—Model results for clouds 12 and 13 on May 27, 1968.

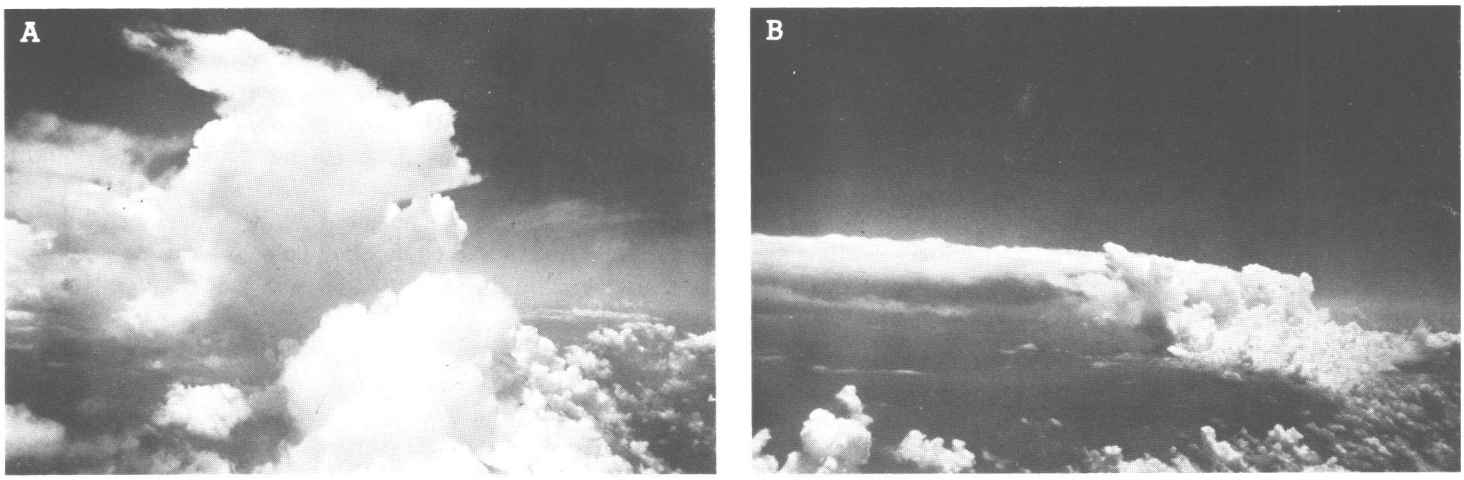

FIGURE 19.—Photographs of cloud 13 (seeded) on May 27, 1968; (A) 6 min after seeding and (B) 1 hr and 44 min after seeding; note the long anvil extending more than 80 mi to the left (east).

sistent complex of clouds lasting in approximately the same spot for more than an hour.

Cloud 13 (seeded, fig. 19) was also two-towered and resembled the control cloud except for higher growth and a longer persistence, which was at least 2 hr.

Both seeded and control clouds on this day were very low on precipitation, from both foil sampler and radar measurements. The seeded cloud was the second driest of the experiment, producing only 87.8 acre-ft of rain in the 40 min following seeding. The control cloud produced only 17.3 acre-ft so that ΔR was still appreciable, namely 70.5 acre-ft, in fair correspondence with the seedability (straight line in fig. 7).

On figure 18, we see that the model fallouts of precipitation from both seeded and unseeded towers are large

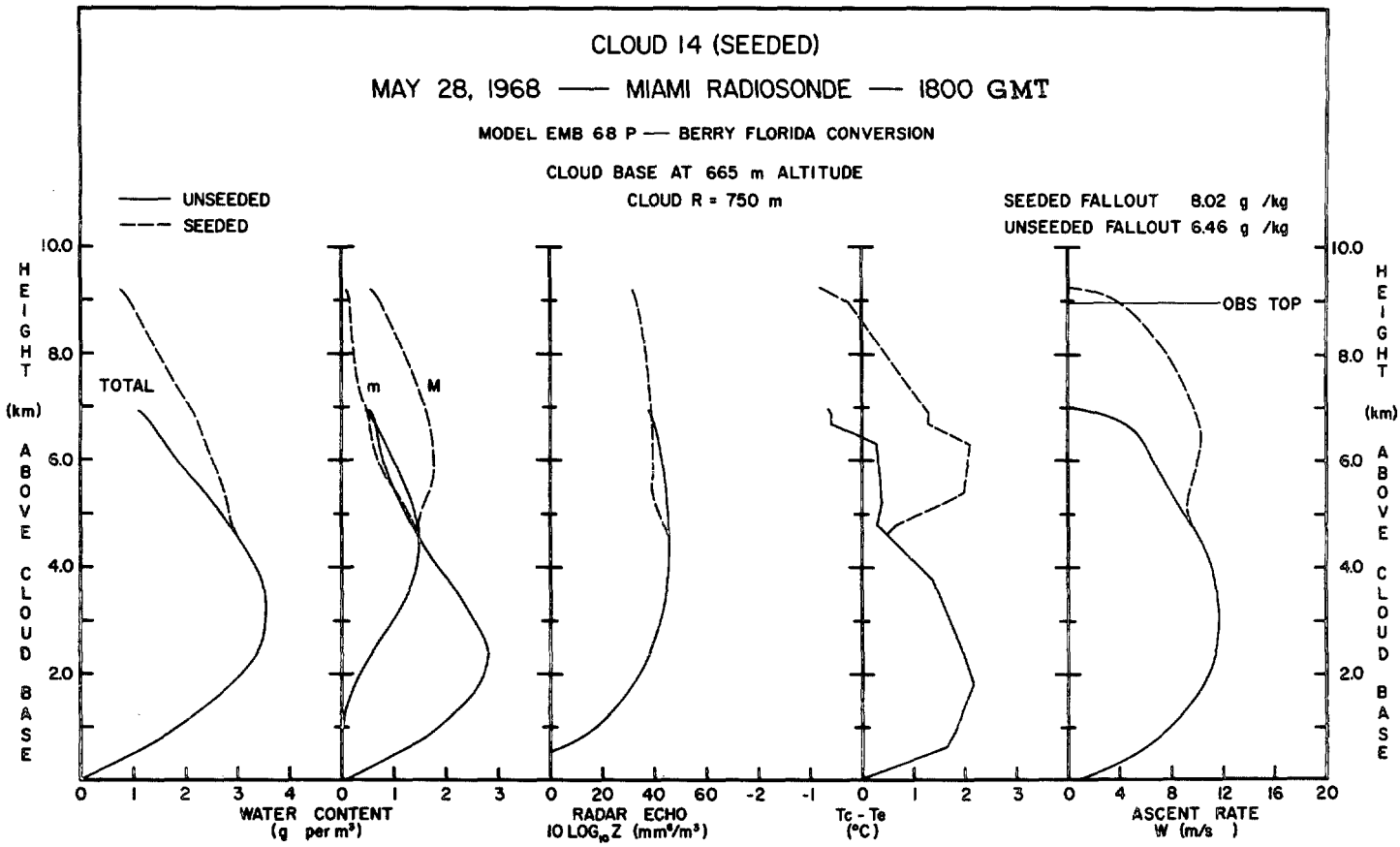

FIGURE 20.—Model results for cloud 14 on May 28, 1968.

and comparable to the seeded fallouts on the early days of the experiment. We hypothesize that the reason for the smaller precipitation actually falling from the May 27 clouds was combined wind shear and dry surroundings. The precipitation particles produced by the active towers probably were both exported in the anvils and also, because of the slant, fell outside the cloud bodies and evaporated rather than being able to grow by coalescence during fall through cloud. Coalescence growth is discussed more fully in section 7.

MAY 28 (FIG. 20)

This day was a poor one for the experiment due to a disturbance over the area. The aircraft had to work over the Florida Peninsula in a region where natural convection was rampant, with many cumulonimbi growing naturally to above 40,000 ft. Other permitted areas were precluded either by the presence of stratus layers or the absence of seedable clouds.

The real time model prediction showed that all radii of 1000 m and above would grow to above 11 km naturally. *Cloud 14* (seeded) was actually the second narrowest of the experiment with a radius of 750 m. The cloud was a member of a line oriented from south-southwest to north-northeast. About 10 mi to the north-northeast of the selected cloud, a large cumulonimbus towered above 40,000 ft without, however, covering the GO cloud with its anvil.

Predicted and observed seeded tops were in fair agree ment (fig 20). Few other comparisons with observations could be made for this cloud because of difficulties with the DC–6 penetrations. Due to the many similar-looking towers in the area, the first two DC–6 penetrations were not through the tower selected by the seeder, while the third penetration had to be aborted due to intense in-cloud turbulence. The day's operation was discontinued at that point.

Two radar control clouds were selected on this day for precipitation measurements. As shown in table 4, there was virtually no difference in rainfall from seeded and control clouds; and all three clouds were among the driest studied.

MAY 30 (FIGS. 21 THROUGH 27)

This was one of the most interesting and informative days of the experiment. The South Florida weather was still very disturbed, with broken cirrus overhead and extensive convective cloudiness, lined up with the wind shear (from southwest). The magnitude of the shear vector (4,000–35,000 ft) was 52 kt, the second largest in the program. Nevertheless, it was possible to select fairly isolated cumuli for the experiment, and four GO clouds were studied; one was a control, and three were seeded.

As seen in table 4, this was the only day on which both model-predicted and observed precipitation changes (Δr and ΔR, respectively) showed negative values. All GO

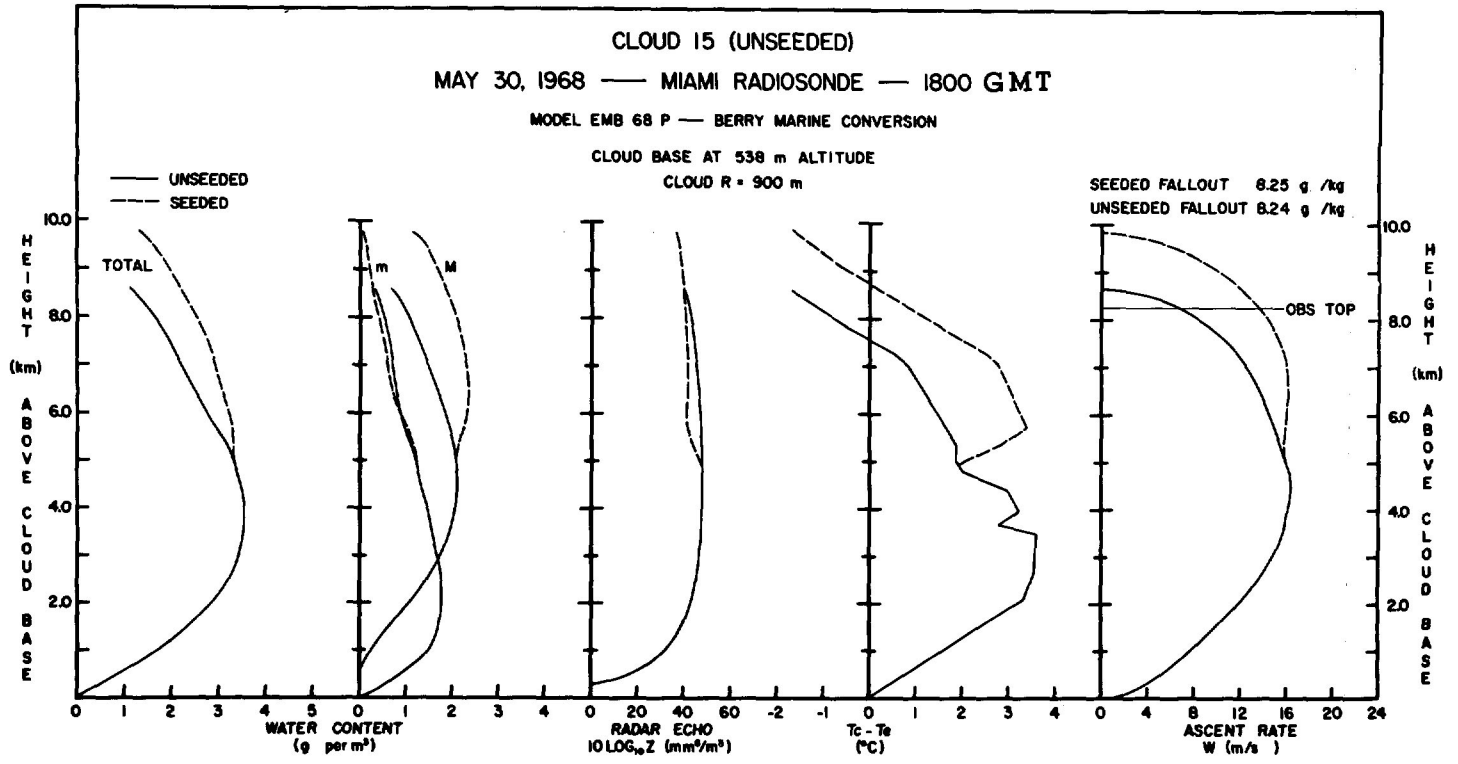

FIGURE 21.—Model results for cloud 15 on May 30, 1968.

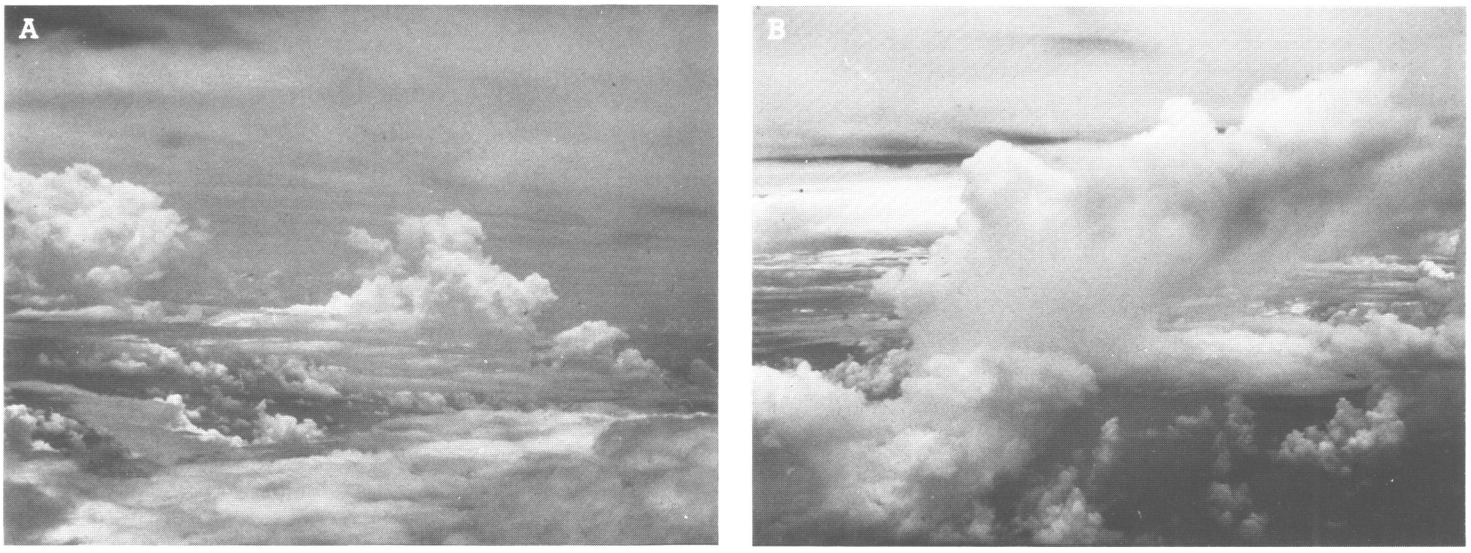

FIGURE 22.—Photographs of cloud 15 (control) on May 30, 1968; (A) 10 min before seeding run and (B) about 10 min after seeding run, looking northwest. Note steep slant, weak cloud body, and the tower precipitation falling outside the cloud.

clouds were fairly wet, producing from about 100 to about 400 acre-ft of rainfall in the 40 min after the seeding run.

Cloud 15 (control, figs. 21 and 22) and *cloud 16* (seeded, figs. 23 and 24) grew over Florida Bay and were an almost perfect pair, with the same environment, the same physical appearance, and nearly the same radius. Cloud 15 was the highest and much the wettest control cloud of the program, reaching 32,000 ft and precipitating 305.9 acre-ft in the 40 min following the "seeding" run. We believe it was typical of the natural medium-to-large cumuli over Florida on this day.

Cloud 16 (seeded) reached only 1000 ft higher than unseeded cloud 15 and precipitated 105.2 acre-ft less (table 4). Figure 23 shows that it topped about half way between the heights of the predicted unseeded and predicted seeded tops. We believe that the seeding was not very effective in invigorating the whole cloud dynamically, hence it failed to grow to the full seeded height and rained less

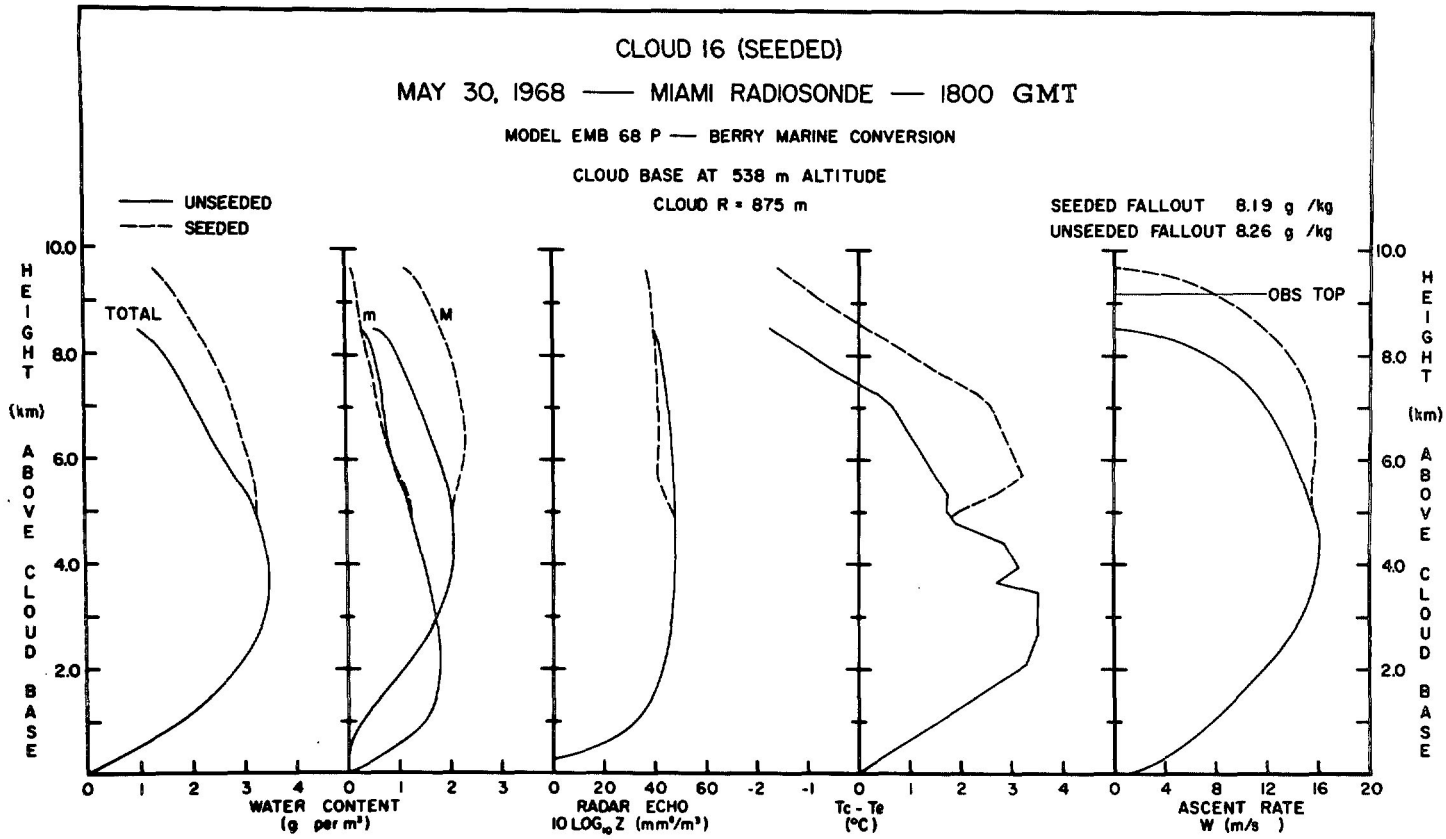

FIGURE 23.—Model results for cloud 16 on May 30, 1968.

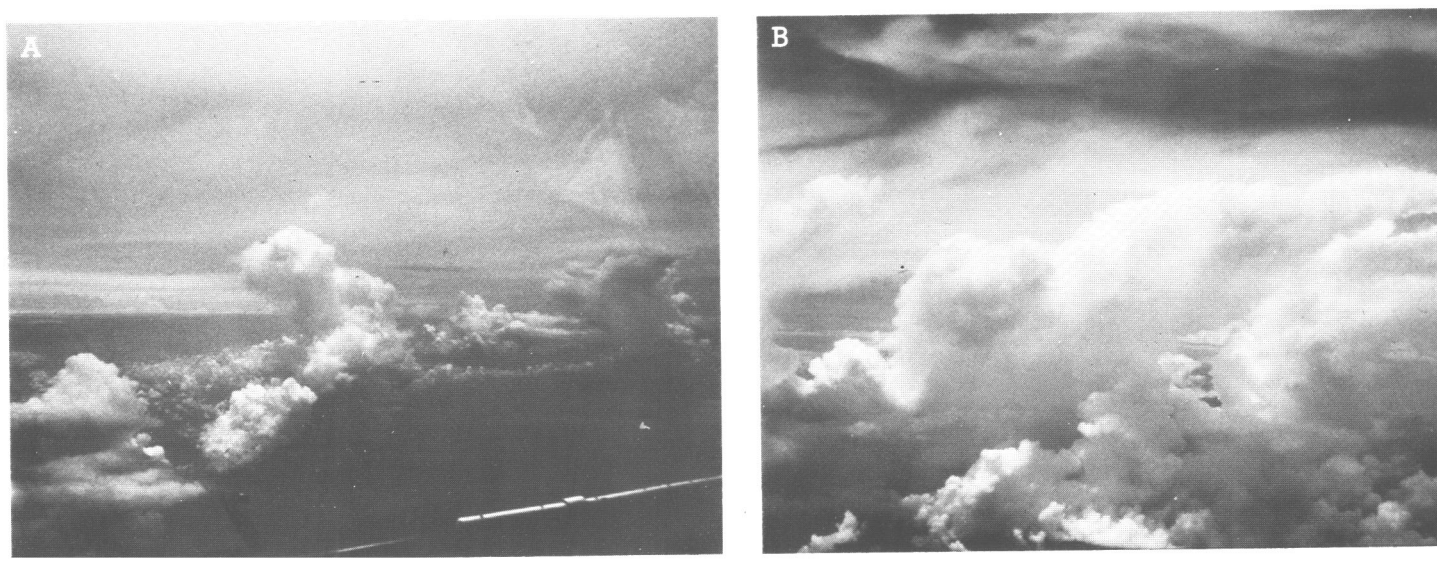

FIGURE 24.—Photographs of cloud 16 (seeded) on May 30, 1968; (A) 10 min before seeding, looking southeast; note slant of tower; (B) 14 min after seeding, looking northwest; note similarity to cloud 15, figure 22B.

rather than more than the control. The hypothesized reason for the failure is illustrated by comparing figure 24A with figure 9A. In the early part of the program, the clouds were growing mainly vertically. Hence, new towers were close to the older ones horizontally and would be seeded by the seeder aircraft on almost any course; furthermore, seeding material falling down through the tallest tower at seeding time would encounter the newer ones coming up beneath it. With strong shear, the old towers are swept away horizontally so that, when seeding the highest tower, the seeder would not seed the newer ones unless he flew directly along the shear vector (as he did not with cloud 16). Figure 24A, made 10 min before seeding, shows the top tower already displaced laterally so far that much of the material dropped in it would fall through to clear air, rather than infecting new towers that are growing quite far

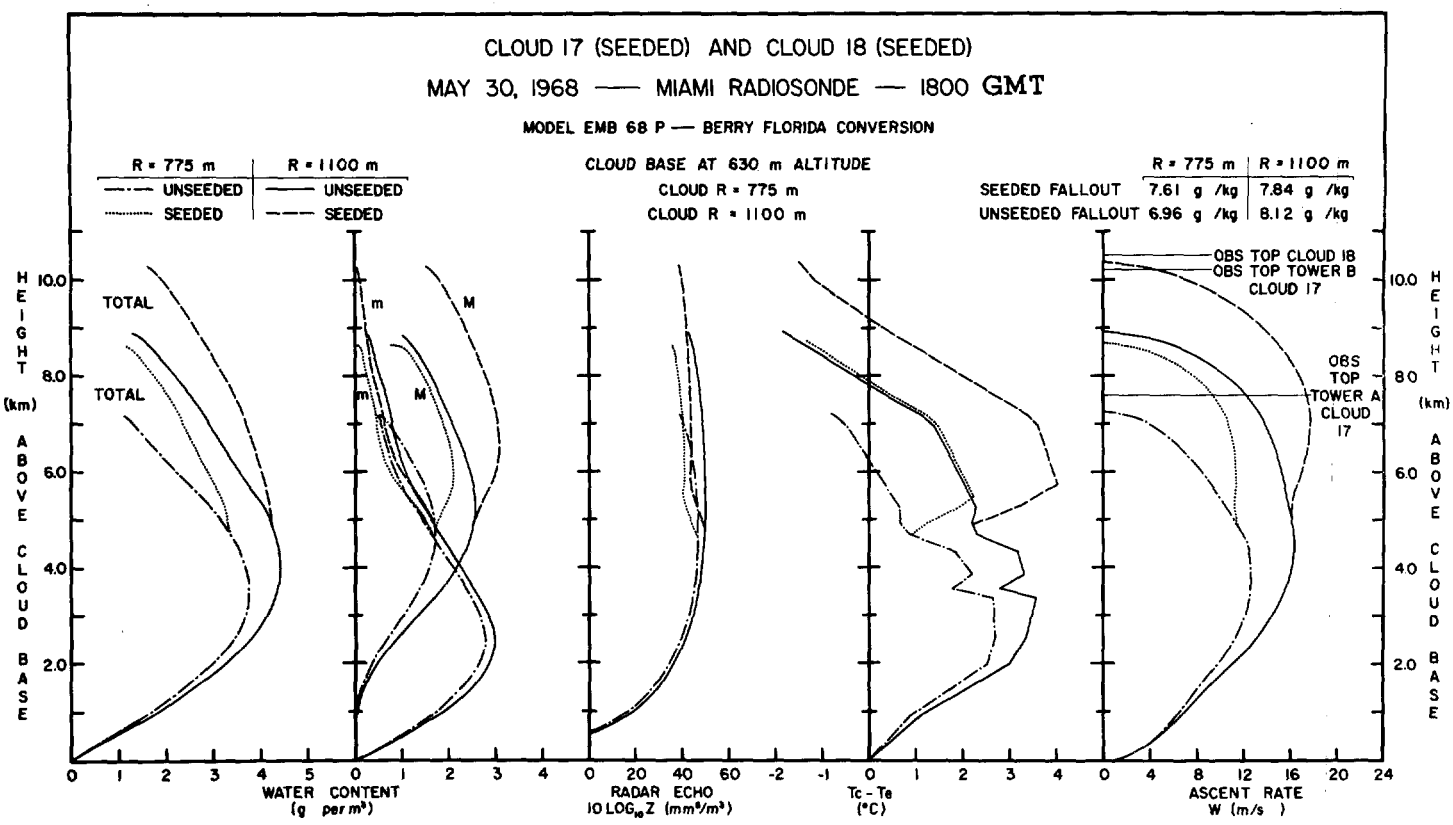

FIGURE 25.—Model results for clouds 17 and 18 on May 30, 1968. Tower A of cloud 17 is shown by the dash-dotted and dotted curves. Tower B of cloud 17 and of cloud 18 are shown by the solid and dashed curves.

to the right. We explain the decreased precipitation, relative to cloud 15, as due to more particles being "hung up" in ice forms and being exported laterally in the anvil, without the usual overcompensating invigoration of the condensation and coalescence process. The model predicts a fallout decrease from the seeded tower even if it had attained its full predicted height. This decrease results mainly from the large height attained by the unseeded tower. Of course, had the seeded cloud truly exploded, successive towers could have overcome the decrease predicted for the first one; however, in the case of cloud 16, explosion failed to occur for the reasons cited above.

Cloud 17 (figs. 25 and 26) was the most extreme case of hesitation growth in the program. It is the subject of an entire report by Woodley and Powell (1970) and will only be summarized briefly here. The tower seeded (tower A) was very narrow; it was seeded only after it had stopped growing and had begun to descend and dissipate. From figure 25, we see that this tower failed to attain its predicted seeded growth, due probably to a combination of late seeding and destruction from penetration by three heavy aircraft. Fortunately for cloud 17, tower A stopped growing at about 9 km or below the strong shear layer, so that its remains hung over the cloud body where new towers were growing (fig. 26B). Beginning at about 12 min after seeding (fig. 26C), a new 1100-m tower (B) started to grow up from the cloud body into the dissipated remnants of tower A, following which the whole cloud grew explosively. Woodley and Powell (1970) have described the cloud's growth in detail, including a comparison of predicted (seeded) and observed rise rates in which agreement was found to be very good. This cloud provided one of the few opportunities to compare predicted and observed temperature excesses, which also agree within the uncertainty of sampling and measurement. The dashed curve in figure 25 shows that the predicted seeded top of an 1100-m tower and the observed final top of tower B of cloud 17 are in excellent agreement, confirming that B was seeded by the silver iodide and ice crystals falling out of the remnants of A. Whether or not the seeding was responsible for the initial formation of the larger tower cannot be determined; if so, seeding can have a much more potent and more complex effect upon cumuli than any simplified model such as ours can hope to treat. The rainfall study showed that cloud 17 precipitated 88.1 acre-ft more (table 4) than control cloud 15, a result clearly attributable to the multiple towers.

Cloud 18 (figs. 25 and 27) was the only typical exploding cloud on May 30. The first tower sighted (at the left in fig. 27A made at seeding time) was at nearly 30,000 ft, and considered too high for seeding. It later blew off and died without further growth. The new upshear tower on the southwest (center of fig. 27A) was seeded and subsequently grew to above 10 km (fig. 27B), in good agreement with the predicted seeded top. Then the whole cloud grew explosively to cumulonimbus stature (fig. 27C). Because of the high predicted and observed unseeded tops, it is not certain that the explosion can be attributed to the seeding. However, the cloud had a more than 46-min history of observation before seeding in

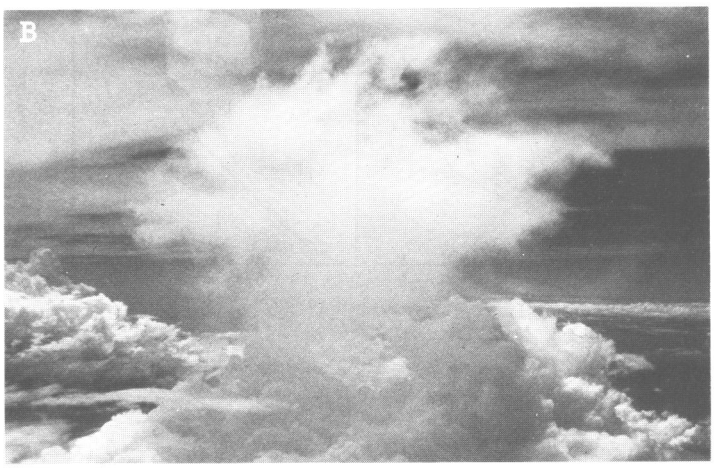

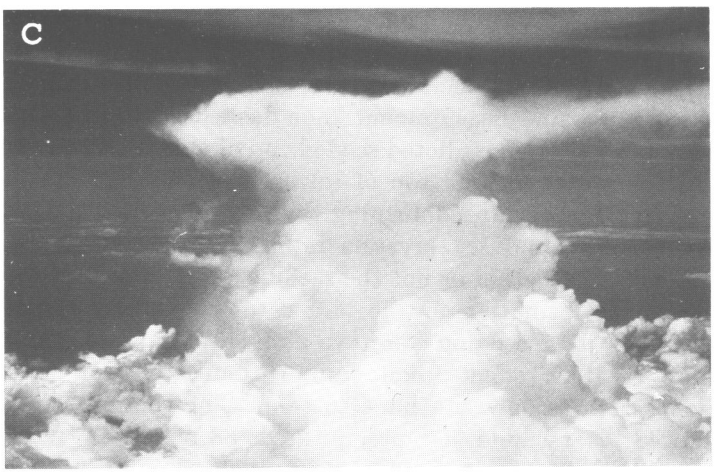

FIGURE 26.—Photographs of cloud 17 (seeded) on May 30, 1968; (A) cloud at second seeding, showing tower A; (B) 10 min after seeding, showing remains of tower A suspended over cloud body where new towers are growing; (C) 13 min after seeding, cloud starting to regenerate; tower B is seen growing up into remnants of tower A.

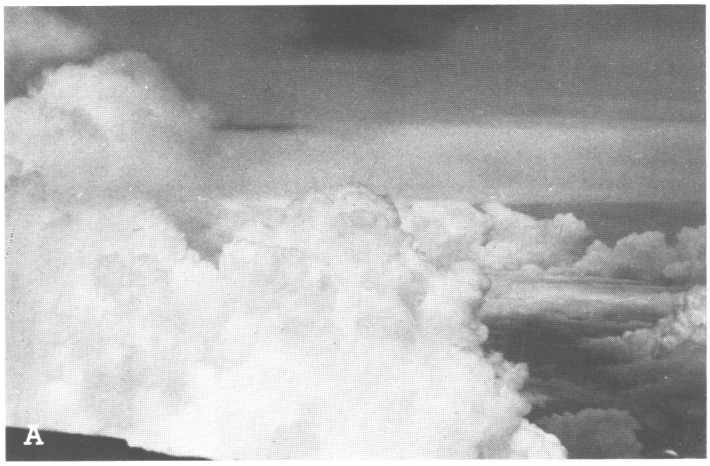

FIGURE 27.—Photographs of cloud 18 (seeded) on May 30, 1968; (A) at seeding time; seeded tower in center, older unseeded tower to left (northeast); (B) 10 min after seeding, looking northwest; seeded tower exploding; older unseeded tower is seen dissipating on the right; (C) 31 min after seeding, looking north; cloud has exploded; cloud 17 is visible in the background to the right (northeast).

which it did not explode. Furthermore, the only other cumulonimbus in the vicinity was seeded cloud 17 (visible on the right in fig. 27C). Despite the many towers, the radar measurements on cloud 18 showed a rainfall deficit of 198.6 acre-ft relative to cloud 15. However, cloud 18 spent much of its seeded life in the blind cone of the radar; and Woodley (1970*a*) suggests that its seeded rainfall may have been underestimated by as much as a factor of 4.

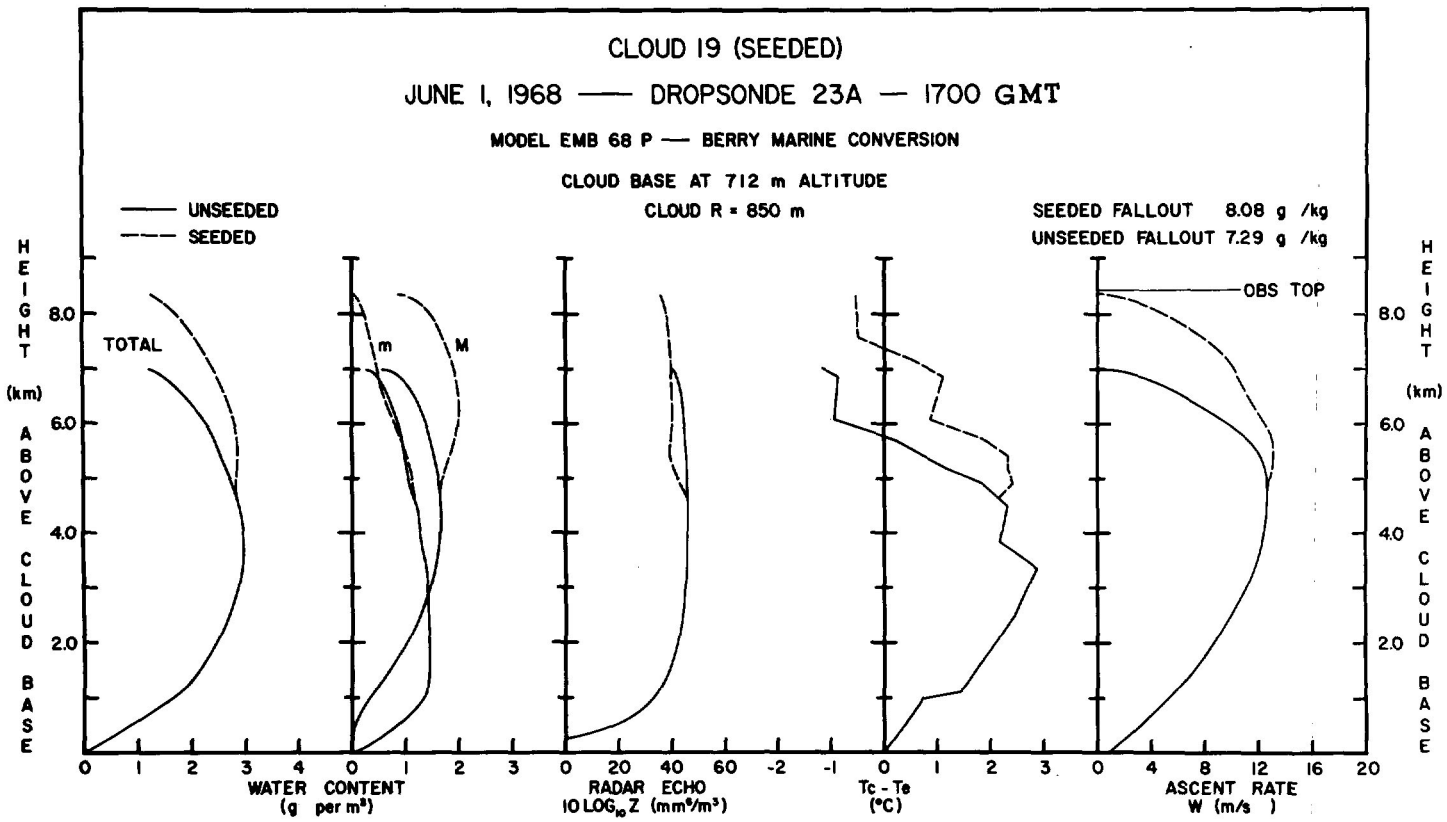

FIGURE 28.—Model results for cloud 19 on June 1, 1968.

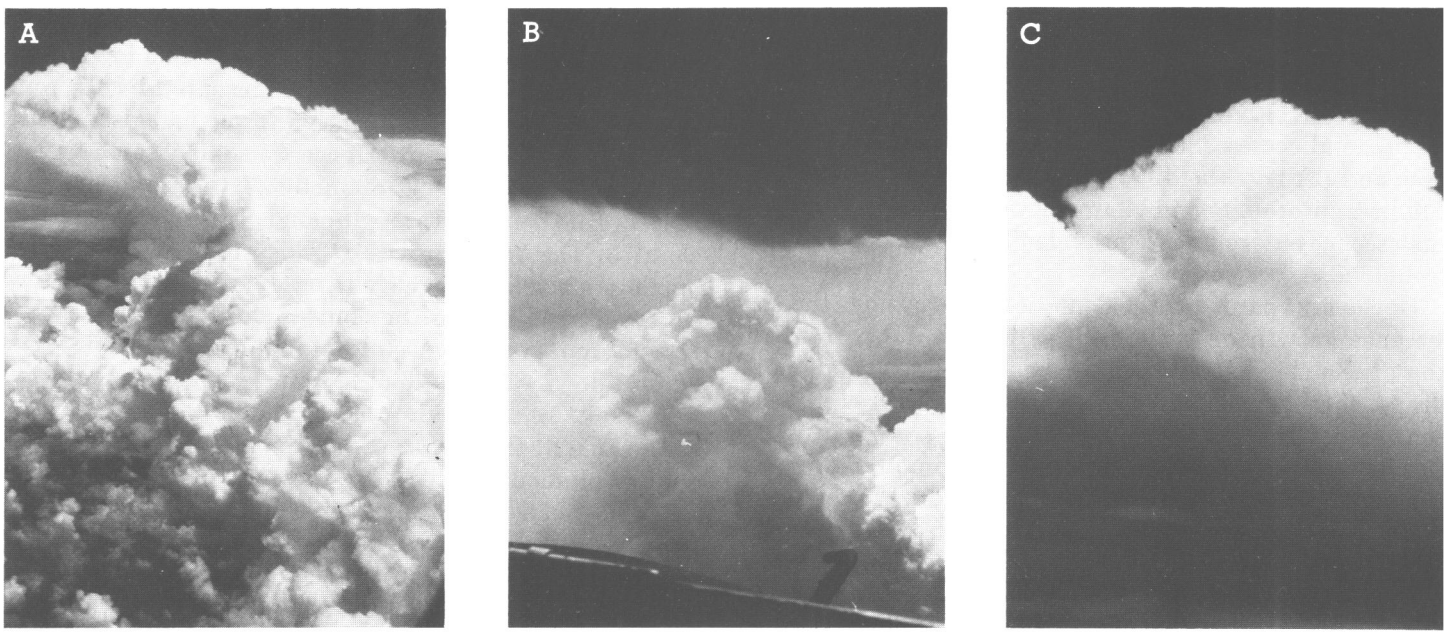

FIGURE 29.—Photographs of cloud 19 (seeded) on June 1, 1968 (by William Woodley); (A) cloud 46 min before seeding; it retained this appearance until seeding; (B) seeded tower 6 min before seeding: and (C) seeded cloud 22 min after seeding; note the growth of the seeded tower that is now dominating the cloud.

JUNE 1 (FIGS. 28 AND 29)

This day continued to be a strong shear day, with highly disturbed weather over the Florida Peninsula. The land areas were, in fact, so much covered by stratus layers that the aircraft had to proceed nearly 180 mi into the Gulf of Mexico off the Florida west coast to find a seedable cloud.

Cloud 19 formed in the clear air at the marine location shown in figure 1. It was studied for nearly 2 hr prior to seeding, during which it remained in a steady state in the same location while putting up a succession of similar

towers and retaining the appearance shown in figure 29A. All unseeded towers had approximately the same horizontal dimensions and topped below 8 km.

The seeded tower at 6 min before seeding is shown in figure 29B. Following seeding, it grew to about 1.4 km above the unseeded tops, in good agreement with the model (fig. 28). By 24 min after seeding (fig. 29C), the seeded tower had expanded and was beginning to dominate the whole cloud, which was dynamically invigorated to some extent. The degree of explosion was, however, limited by the wind shear well below those observed in the early days of the experiment.

Since the cloud was out of the 100-mi range of the University of Miami radar, no rainfall calculations were possible. No aircraft penetration data were available for this case due to instrumental and recording system failures.

7. GROWTH BY COALESCENCE OF THE FALLING PRECIPITATION

In each model calculation (figs. 8, 10–12, 15–18, 20–21, 23, 25, and 28) the seeded and unseeded tower fallouts of precipitation were printed (in g kg^{-1}) in the upper right portion of each diagram. In section 5, we pointed out that the measured precipitation at cloud base, while well correlated with these numbers, exceeded them in magnitude by many factors. This is because the model so far only computes the precipitation falling out of the active tower as it rises. The discrepancy occurs because these precipitation particles grow by coalescence as they fall down through the cloud body.

Here we undertake a coalescence calculation to illustrate two points: (1) how the model-computed fallout can grow by in-cloud coalescence to the amounts observed at cloud base and (2) how the differences between seeded and control precipitation amounts are augmented by the different coalescence environments provided by the seeded and control clouds.

In the first part of this calculation, we consider the coalescence growth of a raindrop as it falls down from the top of the cloud to cloud base, collecting the small cloud drops that it encounters. In this simplified approach, coalescence is regarded as a continuous process in which the small droplets, of constant size and number, are visualized as filling space with a uniform density of liquid water that the large drops sweep up continuously. In this "continuous collection" model, all the large drops grow at the same rate given by

$$\frac{dR}{dt}=\frac{\pi}{3}\int_0^R n(r)r^3E(R, r)[v(R)-v(r)]dr \qquad (12)$$

where $n(r)dr$ is the number of droplets per unit volume of air with radii between r and $r+dr$ and where $E(R, r)$ is the collection efficiency for two droplets of radii R and r and terminal velocities $v(R)$ and $v(r)$, respectively. In the simple case where all the small droplets have the same size and together constitute a water content of m grams per unit volume of air, eq (12) reduces to

$$\frac{dR}{dt}=\frac{E(R, r)}{4\rho_L}m[v(R)-v(r)] \qquad (13)$$

where ρ_L is the density of water.

In our model, we assume $E=1$ for both water and ice; we neglect $v(r)$ and assume $\rho_L\approx 1$. Therefore, when multiplied through by dt, eq (13) becomes

$$dR=\frac{m}{4}v(R)dt=\frac{m}{4}dz \qquad (14)$$

or

$$\Delta D=\frac{m}{2}\Delta z \qquad (15)$$

where D is raindrop diameter and the descent of the drop is divided into height intervals Δz over which a constant value of m can be assumed.

For this calculation, we consider the growth of the volume median precipitation drop with diameter $D_0(z)$ in the radar control cloud on May 16 and in seeded cloud 3 on the same day. This case represents both the rainiest seeded cloud and the largest measured precipitation difference between a seeded and a control cloud. We take two essential parts from observations. First, extensive measurements are available for D_0 at cloud base in both seeded and unseeded clouds from a foil sampler[5] flown by the NRL S2D aircraft. The average D_0 for 15 unseeded passes was 3.14 mm and for 20 seeded passes 3.72 mm. Second, the EMB 68 P model gave values of D_0 at DC–6 level (about 6 km) that agreed well with those measured by the foil in every case, even when the active tower had risen considerably above the aircraft. Hence we shall assume that the model gives the starting diameter of the raindrops when they begin their fall through cloud. In the case of seeded cloud 3, the model gives $D_0=0.8$ mm at 11 km, the maximum height (above cloud base) achieved by the tower center. In the case of the control cloud, the model gives $D_0=1.7$ mm at the highest level (6 km). We then integrate eq (15) downward to cloud base in 1-km steps, with input and results as shown in tables 8 and 9.

In table 8, the values of m are chosen as follows. The computed model value (for the active tower) is taken down to that height interval 6–5 km where the value exceeds 0.8 g m^{-3}. Below that, m is taken constant at 0.8 g m^{-3}, with the idea that the precipitation is falling through an inactive cloud rather than the rising tower. The values in table 8 are considered reasonable figures from our hot wire measurements, for inactive cloud matter at the periphery of the updraft. In table 9, $m=0.48$ g m^{-3} was the model value in the interval 6–5 km; it was considered the maximum reasonable for such a small unseeded cloud,

[5] At this writing, there is still some question regarding the very largest drops apparently measured by the foil sampler at cloud base, both in regard to instrument calibration and possible distortion of drop imprint by aircraft or other effects. It is readily shown, however, that the inclusion or exclusion of these few very large drops makes only a small difference in the volume median diameters.

TABLE 8.—*Collection calculation, seeded cloud 3 on May 16, 1968*

1 Level (km above base)	2 m (cloud water) (g m^{-3})	3 Drop D_0 (precipitation) (mm)	4 Increase in drop mass (%)
11		0.8	
	0.06		11
10		.83	
	.13		27
9		.9	
	.18		37
8		1.0	
	.23		33
7		1.1	
	.40		65
6		1.3	
	.80		123
5		1.7	
	.80		88
4		2.1	
	.80		69
3		2.5	
	.80		56
2		2.9	
	.80		47
1		3.3	
	.80		41
0 (base)		3.7	

TABLE 9.—*Collection calculation, radar control cloud on May 16, 1968*

1 Level (km above base)	2 m (cloud water) (g m^{-3})	3 Drop D_0 (precipitation) (mm)	4 Increase in drop mass (%)
6		1.70	
	0.48		48
5		1.94	
	.48		41
4		2.18	
	.48		37
3		2.42	
	.48		33
2		2.66	
	.48		30
1		2.90	
	.48		27
0		3.14	

again guided by our hot wire measurements. Clearly, the chosen values of m have also been guided by the necessity for the raindrops to achieve their measured sizes at cloud base level. The last column of tables 8 and 9 contain the figures necessary for the next part of the calculation, namely the percent increase in drop mass in each interval. This increase is found from two successive values of D_0 by taking their ratio, cubing it, multiplying by 100, and subtracting 100. For example, for the first interval in table 9:

$$\frac{1.94}{1.70}=1.14;\quad (1.14)^3=1.48\times 100=148\%;$$

$$148\%-100\%=48\%\text{ mass increment.}$$

These resulting percentage increments are now used with the model-computed fallouts to calculate cloud base precipitation as illustrated in figure 30 and tables 10 and 11. The calculation will be explained using table 10.

The EMB 68 model series gives the precipitation fallout from the active rising tower in each height interval in grams of water per kilogram of cloudy air. This figure is given for 1-km height intervals in column 3. With this figure, columns 2 and 4 are used to obtain column 5, the fallout mass in grams. Then it is assumed that somehow half this precipitation mass is lost by falling out of the cloud (fig. 30) so that column 6 gives half the values in column 5. Column 7 gives the result of the calculation, namely the total precipitation mass after coalescence and addition of fallout that has accumulated after each interval of fall. The procedure is best illustrated by considering the interval 10 to 9 km. Here, 1.54×10^9 g fall into the box from above. This amount will be augmented by 27 percent by coalescence (table 8), so we have

$$1.54\times10^9\times1.27=1.95\times10^9.$$

Then we have a fallout addition of 1.46×10^9 g in the interval. If we assume this enters, in the mean, halfway through the interval, its percentage augmentation by coalescence should be half that of the mass coming from above or 13.5 percent. Thus we should also have

$$1.46\times10^9\times1.135=1.66\times10^9,$$

so that the accumulated mass reaching 9 km is

$$(1.95+1.66)\times10^9\text{ g}=3.61\times10^9\text{ g}$$

as given in the table.

We see, even with losing half the fallout, that the precipitation in the cloud is augmented by a factor of 19 by coalescence and that 630×10^9 g or 512 acre-ft fall out from its base. The corresponding calculation for the control cloud is given in table 11.

Due to its smaller vertical thickness, coalescence in the control cloud augments the tower fallout by only about a factor of 2, to about 23 acre-ft of rain. The question might be raised, considering the addition of fallout with a different drop size in each interval, how good an approximation to observed D_0's in the cloud would be the values in column 3 in tables 8 and 9. This question is readily answered for the seeded cloud with reference to columns 6 and 7 in table 10. By the time the raindrops have descended to 7 km, we see that the ratio of new fallout to already descending mass is only about 24 percent, diminishing to 12 percent in the next interval and thereafter becoming a negligible contribution. The model printout shows that down to 7 km, the D_0 of the incoming mass differs from that given by column 3, table 8, by less than 5 percent. Although the departure becomes progressively larger below this level, it does not matter because of the percentually small contribution of the new fallout to the total precipitation. A similar result applies to the

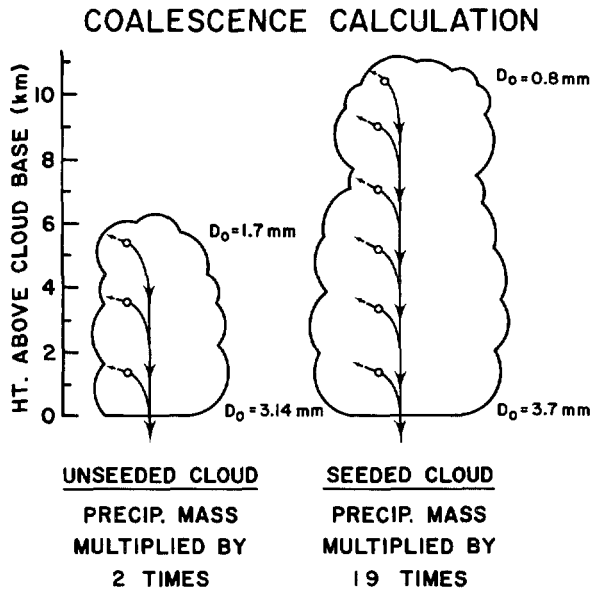

FIGURE 30.—Schematic illustration of coalescence calculation for seeded cloud 3 and the radar control cloud on May 16, 1968.

TABLE 10.—*Precipitation growth calculation for one-tower seeded cloud 3 on May 16, 1968*

1 Level (km above base)	2 Air density $\times 10^3$ g cm^{-3}	3 Calculated fallout EMB 68 P (g kg^{-1})	4 Tower radius R (m)	5 Mass $\times 10^{-9}$ g	6 1/2 mass $\times 10^{-9}$ g	7 Accumulated mass $\times 10^{-9}$ g
11						0
	0.37	0.90	1300	2.93	1.46	
10						1.54
	.41	.81	1300	2.92	1.46	
9						3.61
	.46	.93	1300	3.76	1.88	
8						7.18
	.51	1.11	1300	4.98	2.49	
7						12.45
	.56	1.20	1300	5.91	2.96	
6						24.46
	.63	1.10	1300	6.10	3.05	
5						59.50
	.70	1.16	1000	3.25	1.62	
4						114.19
	.77	.71	1000	2.18	1.09	
3						194.44
	.84	.28	1000	0.94	.47	
2						303.92
	.92	.05	1000	.18	.09	
1						446.87
		~0	1000			
0						
				Sum 33.15	Acc. total	630.09

control cloud. Thus, when making measurements in the rainshaft, we should expect the drop diameters to be dominated by the coalescence in the falling phase and to resemble the distributions of tables 8 and 9. The principal results of these calculations are summarized in table 12.

It will be recalled that the seeded cloud put up two towers (which merged together) in the first 40 min following seeding. Hence this calculation shows that tower fallout, with coalescence on the descent, accounts well for the total seeded precipitation and for the hugely augmented difference in rainfall between seeded and control clouds. These results re-emphasize the importance of the cloud's dynamic invigoration in the rainfall augmentation. It is the greater depth of the cloud produced by the seeding that is responsible for the main part of the precipitation increase, more than 90 percent of which is produced during the descent of the raindrops.

TABLE 11.—*Precipitation growth calculation for the single-tower radar control cloud on May 16, 1968*

1 Level (km above base)	2 Air density $\times 10^3$ g cm^{-3}	3 Calculated fallout EMB 68 P (g kg^{-1})	4 Tower radius R (m)	5 Mass $\times 10^{-9}$ g	6 1/2 mass $\times 10^{-9}$ g	7 Accumulated mass $\times 10^{-9}$ g
6						0
	0.63	2.68	1000	6.75	3.38	
5						4.19
	.70	1.25	1000	3.50	1.75	
4						8.02
	.77	.71	1000	2.19	1.10	
3						12.29
	.84	.28	1000	.94	.47	
2						16.89
	.92	.06	1000	.22	.11	
1						22.21
		0				
0						
				Sum 13.6	Acc. total	28.20

TABLE 12.—*Summary of May 16, 1968, coalescence calculation*

Cloud	Total tower fallout (rising) (acre-ft)	With collection (falling) (acre-ft)	Observed (cloud base) (acre-ft)
Seeded	27 (one tower)	512 (one tower)	850 (two merged towers)
Control (single tower)	11	23	26

In table 10, we see that about 614×10^9 g of the rainfall at cloud base comes from coalesced cloud drops, while only about 16×10^9 g are contributed by raindrops already formed in the rising tower. The question arises as to whether the cloud can readily produce this much cloud water in the 40 min following seeding. We take first a static and then a dynamic approach to this question. On the radar tracing of this cloud's 10-cm echo at 20,000 ft, we define the rainshaft as the area occupied by the third (highest present) contour, which corresponds to a rainfall rate of 0.45 in. hr^{-1} (Woodley 1970*a*). The area enclosed by this contour is 125.5 km^2. With a cloud 11 km tall, we have a shaft volume of about 1.38×10^{12} m^3. For this volume to contain 614×10^9 g of cloud water, the cloud water content must be 0.44 g m^{-3}, a reasonable value. Hence the whole cloud must remain sufficiently vigorous to regenerate itself with roughly this amount of water in this volume about once during 40 min.

A dynamic calculation suggests that the condensation process going on within an area comparable to that of the rainshaft is easily able to regenerate the required cloud water. Let us consider, for example, the height interval from 6–5 km. The cloud gains 32×10^9 g precipitation from coalesced cloud water in this interval (table 10). With wet adiabatic ascent, we would condense about 1.3 g of water per kilogram of rising air in this amount of ascent. The mass of air rising through this level in 40 min, if we assume an updraft of only 50 cm s^{-1}, would be

$$M_{air}=\rho_{air}Aw\,dt$$
$$=0.63\times10^{-3}\times125\times10^{10}\times50\times2400$$
$$=0.95\times10^{14}\text{ g air}$$

and

$$M_{water}=1.3\times10^{-3}\times0.95\times10^{14}=124\times10^9\text{ g water.}$$

This excess over 32×10^9 g allows for a factor of 4 reduction by entrainment, or for the rising air's being confined to a protected region smaller than the area used here. In any case, the spreading of the active tower into an anvil of larger lateral extent appears necessary to allow the falling precipitation particles to have access to the condensation products over an area considerably larger than that of the initial rising tower which has an area of only a few square kilometers. This emphasizes again the importance of the horizontal explosion of the cloud in the precipitation enhancement.

All the foregoing calculations have been made assuming a nearly vertical cloud, so that the precipitation in its descending phase continues to fall through fairly dense cloud matter. After the initial loss of half the fallout from the rising tower, we consider no further losses from the rainshaft. The clouds on May 16 and in all the early part of the program grew almost vertically (e.g. fig. 9), while those in the last half of the program showed extreme slants. In these slanting cases, much of the precipitation will be lost as it will fall outside the cloud body and evaporate rather than grow by coalescence. The photographs in figures 19, 22, and 24 show this loss very graphically. Woodley and Powell (1970) have presented a rough coalescence calculation for cloud 17 on May 30.

8. THE EFFECTS OF SYNOPTIC CONDITIONS UPON SEEDING RESULTS

Every analysis so far points up the subdivision of the experimental period into two quite different synoptic and cloud regimes. During the first part of the program (May 15 through May 20 or May 21), the South Florida region was fair, with isolated cumuli and little or no middle or high cloudiness. During the latter part of the program (from May 26–June 1), a disturbed regime prevailed over South Florida, with rampant convection, much middle and high cloudiness, and abnormally high precipitation. Studies by Fernandez-Partagas (1969) and Woodley et al. (1969) show that the heavy precipitation was natural, due to the presence of the large-scale disturbance, and not demonstrably induced or affected by the seeding, except in the locations of the seeded clouds themselves. Table 13 shows that the results of seeding were quite different in the two periods.

TABLE 13.—*Seeding results in fair (L) versus rainy (S) period*

Parameter	Fair (*L*)	Rainy (*S*)
Average rainfall (ΔR) seeded minus control (in acre-ft)	330	−29
Average seedability (in km) (model EMB 68 P)	3.26	1.67
Average echo duration after seeding (in min)	60	38.6
Average echo area during 40 min after seeding (in n.mi.^{2})	32	16
Average increase in echo area following seeding (in n.mi.^{2})	22	7
Average difference in echo area between seeded and control clouds	16	6

Two main differences in cloud growth were detected between the *L* and *S* periods: (1) unseeded clouds grew an average of 1.2 km higher and (2) seeded clouds showed much less horizontal expansion, or weaker explosion, following seeding in the *S* period.

Mean Miami soundings prepared for the two periods (not reproduced) showed that from cloud base to 8.5 km, or about the height of unseeded tops, the *S* period was 6 percent less stable while from 8.5 km up to 12 km it was 20 percent more stable. In the lower levels, the *S* period was slightly more moist, except for a dry region from 600–500 mb. As discussed in I, a dry layer like this may cause cumuli to break and thereby militates against the horizontal expansion necessary for explosive growth.

A larger difference is found when we compare the mean streamlines for the two periods, shown in figures 31 and 32. Particularly notable is the stronger vertical wind shear in the *S* period, which is even more pronounced when individual days are examined. For example, from May 15–20, the average magnitude of the shear vector between 4,000 and 35,000 ft was 22 kt, while between May 27–30, it averaged 41 kt, nearly a factor of 2 larger. We hypothesize that this was the primary cause of the different seeding results in the two periods. Horizontal cloud explosion is inhibited by strong shear, since succeeding towers do not come up in the protection of previous ones and precipitation growth by coalescence in the cloud body is restricted by loss on the downshear side of a highly slanting cloud. Comparison of the cloud photographs shows nearly vertical clouds in the fair (*L*) period and highly slanting ones occurring in the disturbed (*S*) period. There will of course be fair periods with strong vertical wind shear, and it is planned to study these in future programs to determine whether the shear is the primary restrictive factor rather than merely the presence of the disturbance.

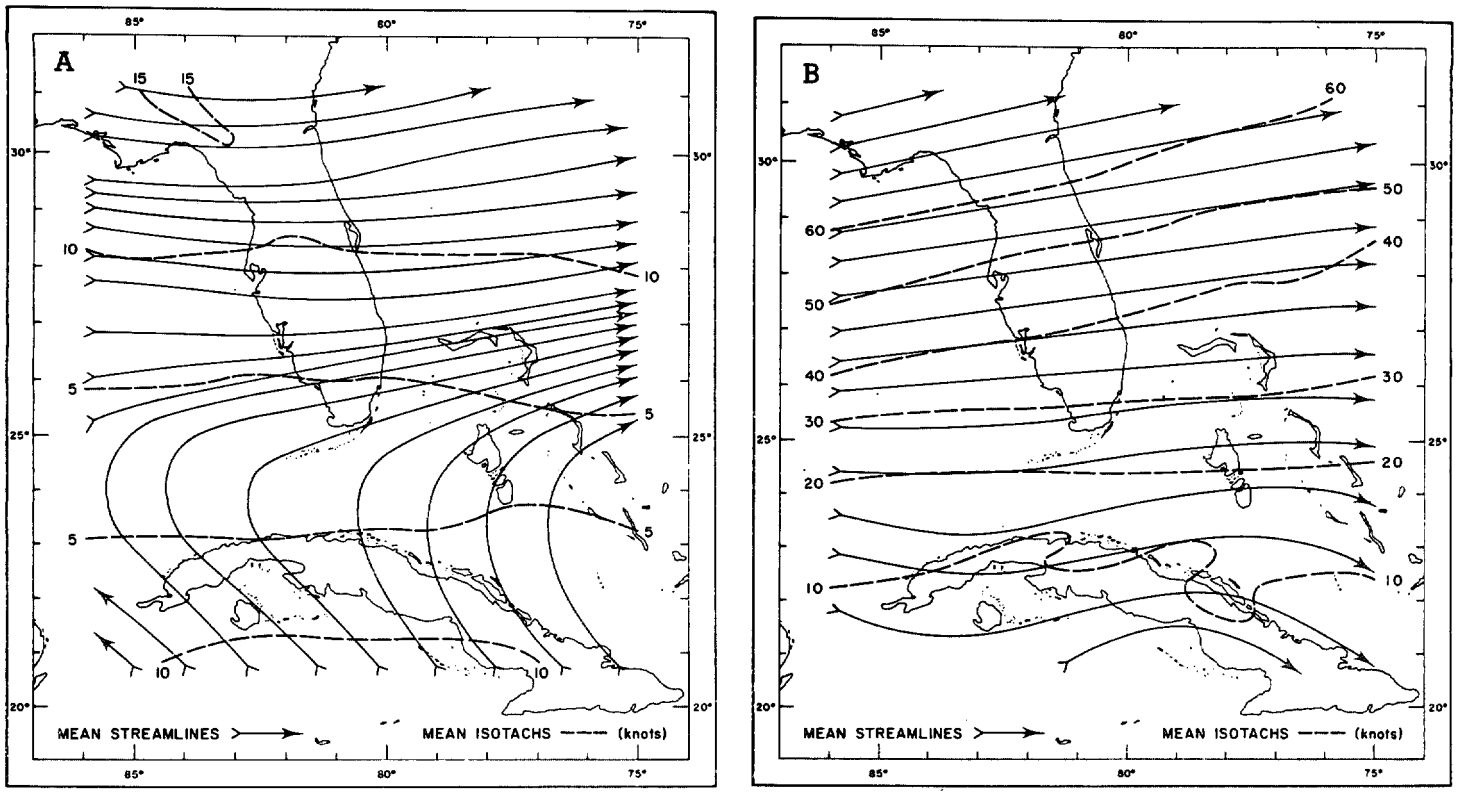

FIGURE 31.—Mean streamlines and isotachs for the fair (*L*) period, extending from 0000 GMT on May 16, 1968, to 0000 GMT on May 22, 1968; (A) 4,000-ft mean streamlines and isotachs and (B) 35,000-ft mean streamlines and isotachs.

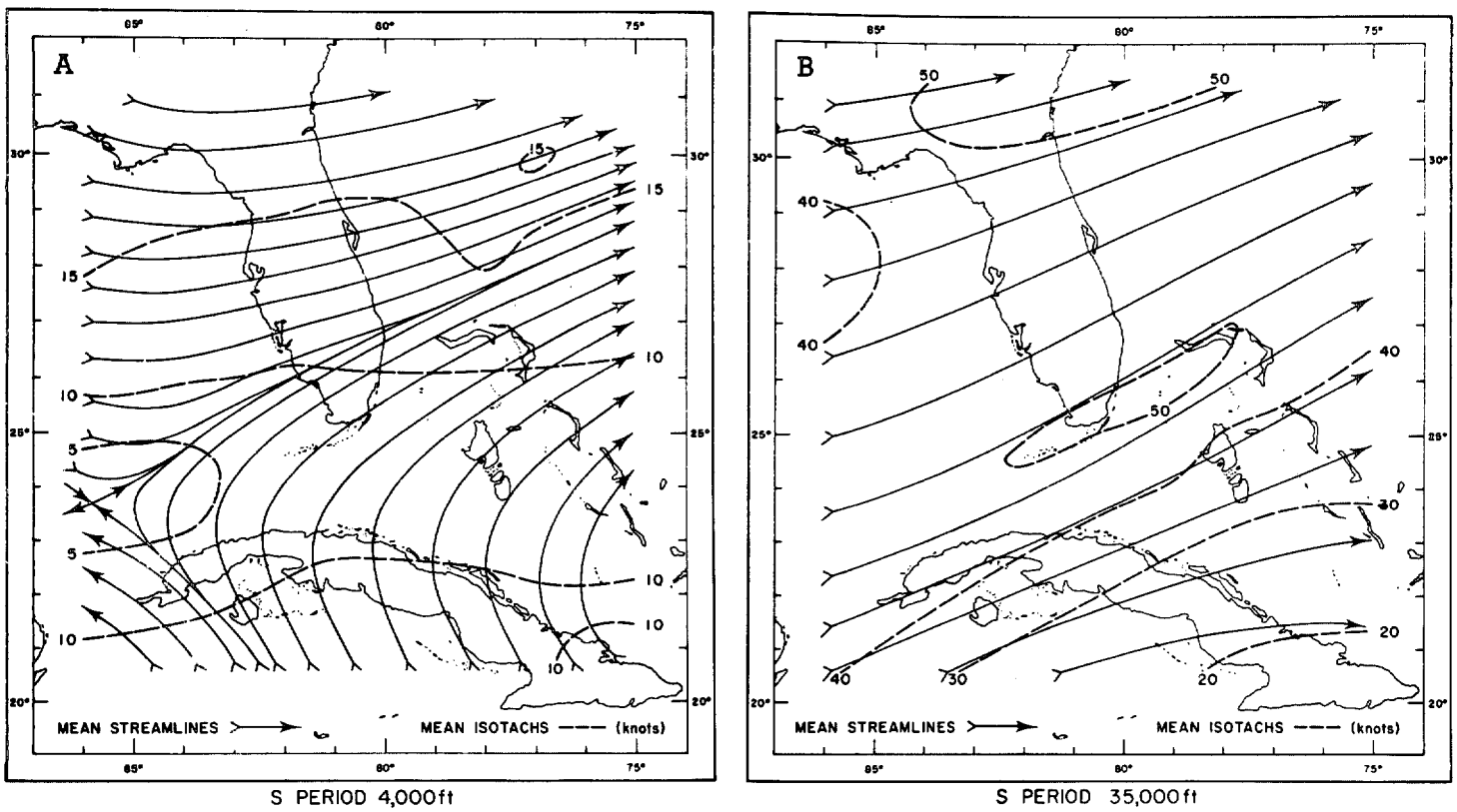

FIGURE 32.—Mean streamlines and isotachs for the disturbed (*S*) period extending from 0000 GMT on May 27, 1968, to 0000 GMT on May 31, 1968; (A) 4,000-ft mean streamlines and isotachs and (B) 35,000-ft mean streamlines and isotachs. Over South Florida, note the asymptote of convergence at low levels and the isotach maximum at high levels.

9. CONCLUSIONS

The EMB 68 model series gives very good height predictions for the 14 GO clouds in the Florida 1968 experiment. When physical measurements from the field program were incorporated into the model to construct the EMB 68 P version, we obtained both good heights and predicted rainfall differences that correlated well with the radar-measured differences between seeded and control clouds. The model calculates only the precipitation falling from the actively rising tower and does not consider further coalescence during the descending phase of the raindrops' lifetime. Hence the model values of precipitation fallout are smaller than the rainfall measured at cloud base (in the 40 min following the seeding run) by factors of about 15–20. A separate prototype coalescence calculation of the descending phase of the rain, starting with the model fallout and using cloud body values from measurements, gives good agreement with observed precipitation amounts.

A particularly valuable correlation is obtained between model-predicted seedability and measured differences in precipitation between seeded and control clouds. An empirical regression was constructed between seedability and rainfall increase which has been used elsewhere (Simpson et al. 1970*a*) in estimating potential applications of dynamic seeding in water management in two important Florida watersheds.

The two main limitations of using this type of model to predict actual seedability in advance lie (1) in predicting the sounding and (2) in predicting the cloud radii. Combined, these limitations comprise essentially the unsolved problem of weather forecasting. However, we have shown that the model can be applied usefully 4–8 hr before a seeding operation in locations and at times where the atmospheric temperature and humidity stratification are fairly uniform and persistent, that is, primarily in the Tropics. Then assuming a hierarchy of typical radii, good days for seeding can be separated from poor days. The poor days comprise both very dry conditions with no seeded growths and disturbed days where natural clouds reach great heights.

A main conclusion from case study comparisons of our model results with observations is that seeding effects are much more complex than the framework of any one-dimensional model can encompass. There are three major complexities:

1. The time dependence of seeding effects. We saw again and again that towers seeded late in their lifetimes often grew little or not at all, while most of the spectacular growths occurred with towers seeded early enough to be actively rising and to contain 1 g m^{-3} or more of water in small cloud drops. A one-dimensional time dependent model is being developed to attack this problem.

2. The possible effect of seeding in generating larger diameter towers than the cloud produced natually. At least two of our case studies indicated that seeding might have had this effect. A two-dimensional and axisymmetric model series based on those devised by Murray (1970) is being developed that may be able to partially investigate this possibility, which will also be studied by further observations.

3. The problem of horizontal cloud explosion following the vertical tower growth and its inhibition by vertical wind shear. One of the most important results of this study was the demonstration that it was probably the high wind shear in the disturbed latter part of our 1968 experiment that inhibited seeded rain production by preventing or reducing the horizontal explosion of the cloud body. We plan eventually to introduce wind shear in a two-dimensional precipitating model of the Murray type, following the pioneering work in the mountain wave situation by Orville (1968). Meanwhile, we shall continue to pursue this problem observationally.

ACKNOWLEDGMENTS

The writers are grateful for the help of Dr. William L. Woodley in the case studies of the 1968 clouds. Messrs. Glenn W. Brier, Thomas Carpenter, and Gerald Cotton of the Meteorology Statistics Group, Atmospheric Resources Laboratory, ESSA, were most helpful in providing a computer program to develop the regressions between rainfall increases, seedability, and unseeded cloud tops. Our thanks are also due to Mr. J. J. Fernandez-Partagas for preparation of the mean streamline and isotach charts for the fair and disturbed periods. Mr. Robert N. Powell ably drafted the figures. Mrs. Suzanne Johnson and Mrs. Peggy M. Lewis prepared the manuscript.

We are indebted for special soundings to the Observations Section, National Hurricane Center; also to the Naval Weather Service Environmental Detachment, Key West, Fla.; and to the Air Weather Service of the U.S. Air Force.

The work herein was supported in part by the Office of Atmospheric Water Resources, Bureau of Reclamation, U.S. Department of the Interior, under Contract 14–06–W–176.

REFERENCES

Andrews, Donald A., "Some Eeffcts of Cloud Seeding in Cumulus Dynamics," M.A. thesis, Department of Meteorology, University of California, Los Angeles, **1964**, 139 pp.

Berry, E. X., "Modification of the Warm Rain Process," *Proceedings of the First National Conference on Weather Modification, Albany, New York, April 28–May 1, 1968*, American Meteorological Society, State University of New York, Albany, **1968**, pp. 81–85.

Braham, R. R., Jr., "What is the Role of Ice in Summer Rainshowers?," *Journal of the Atmospheric Sciences*, Vol. 21, No. 6, Nov. **1964**, pp. 640–645.

Braham, R. R., Jr., "Meteorological Bases for Precipitation Development," *Bulletin of the American Meteorological Society*, Vol. 49, No. 4, Apr. **1968**, pp. 343–353.

Fernandez-Partagas, José J., "The Mean Circulation, Synoptic Disturbances and Rainfall Patterns Over South Florida and Adjacent Areas in May 1968," *Report*, Grant No. E–22–29–69–G, Division of Atmospheric Science, Institute of Marine and Atmospheric Sciences, University of Miami, Coral Gables, Fla., **1969**, 60 pp.

Gerrish, Harold P., and Hiser, Homer W., "Mesoscale Studies of Instability Patterns and Winds in the Tropics," *Report* No. 7, Contract No. DA–36–039 SC–89111, U.S. Army Electronics Laboratories, Fort Monmouth, N.J., Feb. **1965**, 63 pp.

Herrera-Cantilo, L. M., "Aerial Cloud Photogrammetry Based on Doppler Navigation," *Final Report*, Contract No. E-22-2-69(N), Division of Atmospheric Science, Institute of Marine and Atmospheric Sciences, University of Miami, Coral Gables, Fla., **1969**, 65 pp.

Kessler, Edwin, III, "Microphysical Parameters in Relation to Tropical Cloud and Precipitation Distributions and Their Modification," *Geofisica International*, Vol. 5, No. 3, Mexico City D. F., July **1965**, pp. 79–88.

Kessler, Edwin, III, "On the Distribution and Continuity of Water Substance in Atmospheric Circulation," *Meteorological Monographs*, Vol. 10, No. 32, American Meteorological Society, Boston, Mass., Nov. **1969**, 84 pp.

Levine, J., "Spherical Vortex Theory of Bubble-Like Motion in Cumulus Clouds," *Journal of Meteorology*, Vol. 16, No. 6, Dec. **1959**, pp. 653–662.

Levine, J., "The Dynamics of Cumulus Convection in the Trades: A Combined Observational and Theoretical Study," Ph. D. thesis, Department of Meteorology, Massachusetts Institute of Technology, Cambridge, **1965**, 131 pp.

Malkus, Joanne S., "Recent Developments in Studies of Penetrative Convection and an Application to Hurricane Cumulonimbus Towers," *Cumulus Dynamics, Proceedings of the First Conference on Cumulus Convection, Portsmouth, New Hampshire, May 19–22, 1959*, Pergamon Press, New York, **1960**, pp. 65–84.

Malkus, Joanne S., and Simpson, Robert H., "Modification Experiments on Tropical Cumulus Clouds," *Science*, Vol. 145, No. 3632, Aug **1964**, pp. 541–548.

Marshall, J. S., and Palmer, W. McK., "The Distribution of Raindrops With Size," *Journal of Meteorology*, Vol. 5, No. 4, Aug. **1948**, pp. 165–166.

Mee, T. R., and Takeuchi, D. M., "Natural Glaciation and Particle Size Distribution in Marine Tropical Cumuli," *Final Report*, Contract No. E-22-30-68(N), Meteorology Research, Inc., Altadena, Calif., Aug. **1968**, 71 pp.

Murray, F. W., "Numerical Models of a Tropical Cumulus Cloud With Bilateral and Axial Symmetry," *Monthly Weather Review*, Vol. 98, No. 1, Jan. **1970**, pp. 14–28.

Neel, Carr B., "A Heated-Wire Liquid-Water-Content Instrument and Results of Initial Flight Tests in Icing Conditions," *Research Memorandum* RM A54123, U.S. National Advisory Committee for Aeronautics, Washington, D.C., Jan. 20, **1955**, 33 pp.

Orville, H. D., "Ambient Wind Effects on the Initiation and Development of Cumulus Clouds Over Mountains," *Journal of the Atmospheric Sciences*, Vol. 25, No. 3, May **1968**, pp. 385–403.

Ruskin, R. E., Averitt, J. M., Schecter, R. M., Julian, B. G., Wojciechowski, T. A., and Russ, R. G., "Cloud Physics Measurements in AgI Seeded Clouds," Atmospheric Physics Branch, Naval Research Laboratory, Washington, D.C., June **1969**, 7 pp. (unpublished report).

Saunders, P. M., "The Thermodynamics of Saturated Air: A Contribution to the Classical Theory," *Quarterly Journal of the Royal Meteorological Society*, London, England, Vol. 83, No. 357, July **1957**, pp. 342–350.

Simpson, Joanne, "On the Radar Measured Increase in Precipitation Within Ten Minutes Following Seeding," *Journal of Applied Meteorology*, Vol. 9, No. 2, Apr. **1970**, pp. 318–320.

Simpson, Joanne, Brier, Glenn W., and Simpson, Robert H., "Stormfury Cumulus Seeding Experiment 1965: Statistical Analysis and Main Results," *Journal of the Atmospheric Sciences*, Vol. 24, No. 5, Sept. **1967**, pp. 508–521.

Simpson, Joanne, Holle, Ronald L., Wiggert, Victor, and Woodley, William L., "Potential Applications of Tropical Cumulus Seeding," *Proceedings of the Symposium on Tropical Meteorology, Honolulu, Hawaii, June 2-11, 1970*, American Meteorological Society and World Meteorological Organization, Honolulu, **1970***a*, pp. D VII-1—D VII-6.

Simpson, Joanne, Simpson, Robert H., Andrews, Donald A., and Eaton, Max A., "Experimental Cumulus Dynamics," *Reviews of Geophysics*, Vol. 3, No. 3, Aug. **1965**, pp. 387–431.

Simpson, Joanne, and Wiggert, Victor, "Models of Precipitating Cumulus Towers," *Monthly Weather Review*, Vol. 97, No. 7, July **1969**, pp. 471–489.

Simpson, Joanne, and Woodley, William L., "Intensive Study of Three Seeded Clouds on May 16, 1968," *ESSA Technical Memorandum* ERLTM-APCL 8, U.S. Department of Commerce, Boulder, Colo., May **1969**, 42 pp.

Simpson, Joanne, Woodley, William L., Friedman, Howard A., Slusher, Thomas W., Scheffee, R. S., and Steele, Roger L., "An Airborne Pyrotechnic Cloud Seeding System and Its Use," *Journal of Applied Meteorology*, Vol. 9, No. 1, Feb. **1970***b*, pp. 109–122.

Takeuchi, D. M., "Analyses of Hydrometeor Sampler Data for ESSA Cumulus Experiments, Miami, Florida, May 1968," *Final Report*, Contract No. E-22-28-69(N), Meteorology Research, Inc., Altadena, Calif., **1969**, 44 pp.

Woodley, William L., "Precipitation Results From a Pyrotechnic Cumulus Seeding Experiment," *Journal of Applied Meteorology*, Vol. 9, No. 2, Apr. **1970***a*, pp. 242–257.

Woodley, William L., "Rainfall Enhancement by Dynamic Cloud Modification," *Science*, Vol. 170, No. 3954, Oct. 9, **1970***b*, pp. 127–132.

Woodley, William L., and Fernandez-Partagas, José J., "Radar and Photographic Documentation of Convective Developments on May 16, 1968," *ESSA Technical Memorandum* ERLTM-APCL 7, U.S. Department of Commerce, Boulder, Colo., Apr. **1969**, 17 pp.

Woodley, William L., and Herndon, Alan, "A Raingage Evaluation of the Miami Reflectivity-Rainfall Rate Relation," *Journal of Applied Meteorology*, Vol. 9, No. 2, Apr. **1970**, pp. 258–264.

Woodley, William L., Herndon, Alan, and Schwartz, R., "Large-Scale Precipitation Effects of Single Cloud Pyrotechnic Seeding," *ESSA Technical Memorandum* ERLTM-AOML 5, U.S. Department of Commerce, Boulder, Colo., Nov. **1969**, 26 pp.

Woodley, William L., and Powell, Robert N., "Documentation and Implications of the Behavior of Seeded Cloud 17, May 30, 1968," *ESSA Technical Memorandum* ERLTM-AOML 6, U.S. Department of Commerce, Boulder, Colo., Jan. **1970**, 29 pp.

[Received April 3, 1970; revised May 20, 1970]